

# Rethinking land take futures: A cellular automata-based spatial planning approach to model urban expansion and densification under divergent growth scenarios

Anasua Chakraborty<sup>1</sup>, Ahmed Mustafa<sup>2</sup>, Lien Poelmans<sup>3</sup>, Jacques Teller<sup>1</sup>

<sup>1</sup>LEMA, Université de Liège, Belgium

<sup>2</sup>The New School, New York, USA

<sup>3</sup>Environmental Modelling Unit, Flemish Institute for Technological Research, Belgium

**Corresponding author:** A. Chakraborty, [A.chakraborty@uliege.be](mailto:A.chakraborty@uliege.be)

---

This is a non-peer-reviewed preprint submitted to EarthArXiv.

---

## Abstract

Land take—the conversion of greenfield land into built-up areas—poses critical challenges for sustainable urban development. Addressing this issue requires understanding the balance between outward urban expansion and inward urban densification. This study employs a Multinomial Logistic Regression-based Cellular Automata (MNL-CA) model to simulate two different future scenarios of urban development till 2050 in Wallonia, Belgium—a region experiencing rapid urbanisation. The model simulates two contrasting built-up demand scenarios. The first scenario is density-based, which follows a linear extrapolation of historical trends in built-up demand into the future. Conceptually, this scenario represents a gradual slowdown of urban expansion, indicating a shift to densification. The second applies a stress-test scenario in which urban expansion continues steadily through 2050. The results reveal that under the density-based scenario referred to as Business-As-Usual (BAU), expansion rates decrease sharply, stabilising at approximately 0 hectares per day by 2040. This indicates a shift toward compact urban forms, albeit accompanied by a continuous decline in overall demand. By contrast, the growth-based scenario or Growth-As-Usual (GAU) produces ongoing expansion at around 2.5 hectares per day in 2050, highlighting the risks of uncontrolled land consumption. Spatial metrics further demonstrate that the density-based scenario fosters compact and contiguous development, whereas the growth-based scenario results in fragmented urban forms that challenge the resilience of spatial planning policies. By evaluating both scenarios, our model provides a framework for stress-testing long-term development strategies, enabling more robust assessments for sustainable land-use policy.

**Keywords:** Business-As-Usual, Scenario Modelling, Cellular Automata, Spatial Planning, Sustainable Cities and Communities

# 1 Introduction

Urbanisation is rapidly transforming Earth’s landscapes, with significant implications for natural habitats, carbon emissions, and land-use conflicts. Projections indicate that by 2030, urban land cover could increase by over 1.5 million square kilometres, nearly tripling the global urban land area observed in 2000 (Seto et al. (2011), United Nations (2018), Chen et al. (2020)). This expansion is primarily driven by two processes: *urban expansion* and *urban densification*. Urban expansion involves the outward growth of cities, converting natural landscapes into built environments, which fragments ecosystems and reduces agricultural land (Seto et al. (2011), Elmqvist et al. (2013)). In contrast, urban densification involves intensifying land use within existing urban areas, optimising infrastructure and reducing the per capita environmental footprint (Al-Ahmadi et al. (2009), Esposito et al. (2018)). These processes are distinct from each other and change across different regions with distinct environmental, economic, and social impacts (Barros and Balsas (2020), Dewan and Yamaguchi (2009)).

In developing regions like Sub-Saharan Africa and South Asia, urban expansion dominates due to rapid population growth, informal settlements, and weak regulatory enforcement. Conversely, European cities tend to emphasise densification due to land constraints and sustainability goals, as seen in Berlin, Paris, and London (Esposito et al. (2018), Kasanko et al. (2006)). Exceptionally, in many fast-growing urban centres such as Lagos, Karachi, and Dhaka, expansion and densification often occur simultaneously, complicating urban planning strategies (Wang and Kintrea (2021), Ullah and Ibrar (2022)). Due to such complexities, it is essential to develop predictive models that are able to simulate different urban growth scenarios. While such models can promote informed land-use policies, they are often biased towards urban expansion over densification.

Urban growth modelling typically relies on the Business-As-Usual (BAU) scenario, which assumes that urban expansion will slow over time due to planning interventions and natural saturation (Thorne et al. (2013), Kim and Newman (2020)). BAU is particularly relevant for developed cities where compact growth strategies and zoning policies promote densification over uncontrolled sprawl. Nonetheless, this assumption does not hold true universally. In many regions, particularly where land demand remains persistently high, urban expansion continues despite planning efforts, making BAU an overly optimistic projection.

To address this limitation, we introduce the Growth-As-Usual (GAU) scenario, which assumes a continuous or unconstrained urban expansion at a constant rate, without the gradual decline as observed in BAU. GAU serves as a stress-test, evaluating whether current land-use policies and zoning regulations can withstand persistent development pressures (Lathey et al. (2009), Mundia and Aniya (2005)). While BAU considers a controlled, policy-driven transition toward densification, GAU provides a worst-case scenario, testing the resilience of urban planning strategies in areas experiencing relentless suburbanization. Unlike previous studies, which often assume urban expansion will eventually stabilise, GAU explicitly models the consequences of unchecked land consumption, offering a critical perspective for urban policymakers.

These growth scenarios have been simulated based on a Multinomial Logistic Regression (MNL) based Cellular Automata (CA) model. CA is a widely used spatial modelling approach where urban landscapes are represented as dynamic grids of evolving cells, influenced by socio-

economic, geophysical, and accessibility factors (Batty (1997), Vermeiren et al. (2012), Mustafa et al. (2018b)). Unlike traditional CA models that rely on simplistic binary expansion patterns, MNL-CA distinguishes between multiple urban density levels, enabling a more nuanced understanding of the expansion and densification processes (White and Engelen (1997)). Most existing CA-based urban growth models either focus on policy-driven interventions (Liu et al. (2019)) or fail to integrate stress-test scenarios. For instance, Vermeiren et al. (2012) applied logistic regression to predict BAU urban expansion but did not consider dynamic neighbourhood effects. Similarly, Naikoo et al. (2023) modelled probabilistic urban zones but did not explicitly define GAU or stress-test urban policies. In contrast, our study is the first to apply MNL-CA to simulate GAU, providing a novel framework to assess the long-term implications of persistent urban expansion.

Wallonia (Belgium) presents an ideal case study for testing BAU and GAU scenarios due to its unique urbanisation patterns. Since the mid-20th century, the region has experienced rapid suburban expansion, largely driven by transportation network development and housing demand (ESPON (2020)). Despite planning interventions aimed at promoting densification, Wallonia continues to exhibit high land consumption rates, raising concerns about the effectiveness of current zoning policies. Unlike other European regions where urban growth has stabilised, Wallonia remains in a transitional phase, where both expansion and densification actively shape its urban landscape. This persistent demand for land challenges the assumptions of BAU, making GAU an essential tool for stress-testing the region’s spatial planning strategies (Chakraborty et al. (2023)). By applying GAU to Wallonia, we assess whether the region’s zoning regulations and land-use policies can effectively manage continued suburbanization pressures.

This study focuses on developing an MNL-CA model to simulate urban growth based on the following methodological approach:

- Estimating urban built-up demand based on historical trends derived from existing built-up density maps.
- Developing an MNL-CA model to project future urban expansion and densification.
- Simulating urban built-up expansion under both BAU and GAU scenarios until 2050.
- Establishing a baseline framework for future urban growth studies.

The approach is structured throughout our article as: section [Materials & Methodology](#) describing the study area, datasets used, and methods. Section [Results](#) presenting simulation under different growth demand scenarios. Section [Discussion](#) demonstrating the implications of scenarios on existing and future urbanisation. Finally, section [Conclusion](#) identifies the most suitable baseline scenario for future urban growth modelling and its requirement for further research.

## 2 Materials & Methodology

This section on the materials and methodology talks broadly about the following:

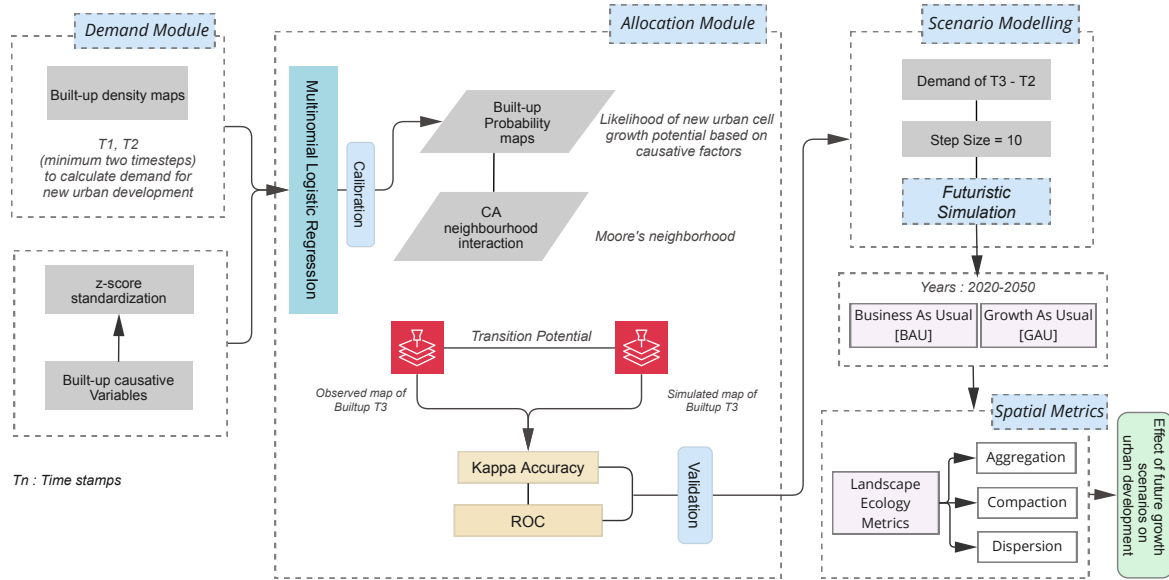


Figure 1: Schema of our study.

1. *Study area* for conducting the research and reason for its selection
2. *Dataset* encompassing the dependent and independent variables impacting urban growth: involves urban expansion and urban densification
3. A detailed *workflow* of the CA modelling for the simulation of future urban growth under a BAU and GAU scenario, as demonstrated in [Figure 1](#)
4. *Spatial metrics* to understand the type of growth under two different scenarios

Thus, the methodology will offer insights into data availability and the potential for replicating similar studies in other research contexts.

## 2.1 Study Area

Wallonia – the southern region of Belgium, covering an area of 16844 km<sup>2</sup>, is selected as our area of study, intriguing urban-rural conurbations ([Figure 2](#)). Wallonia is one of the most densely populated regions in Europe, with 213 inhabitants/km<sup>2</sup>. Due to this growing population and housing demand, the region has experienced high land take since the 1950s. The development of transportation networks has aided people to settle outside the centre, leading to significant urban expansion. This led to the gradual artificialization of areas predominantly by residential uses, at the cost of agricultural lands. As per the report from 2017 ([SPW \(2017\)](#)), artificialization accounts for 1756 km<sup>2</sup>, i.e. 10.4% of the total Wallonia territory.

Additionally, the post-war economic boom and rising household income encouraged suburbanization transitioning people from overcrowded urban centres to wealthier suburbs. Historically, spatial planning in Wallonia relied on rigid zoning laws and hierarchical sector plans ([Hanocq \(2011\)](#)). The policies ([ESPON \(2020\)](#)) aimed to regulate land use but struggled to keep up with rapid urban growth, leading to fragmented development and inefficient land use.

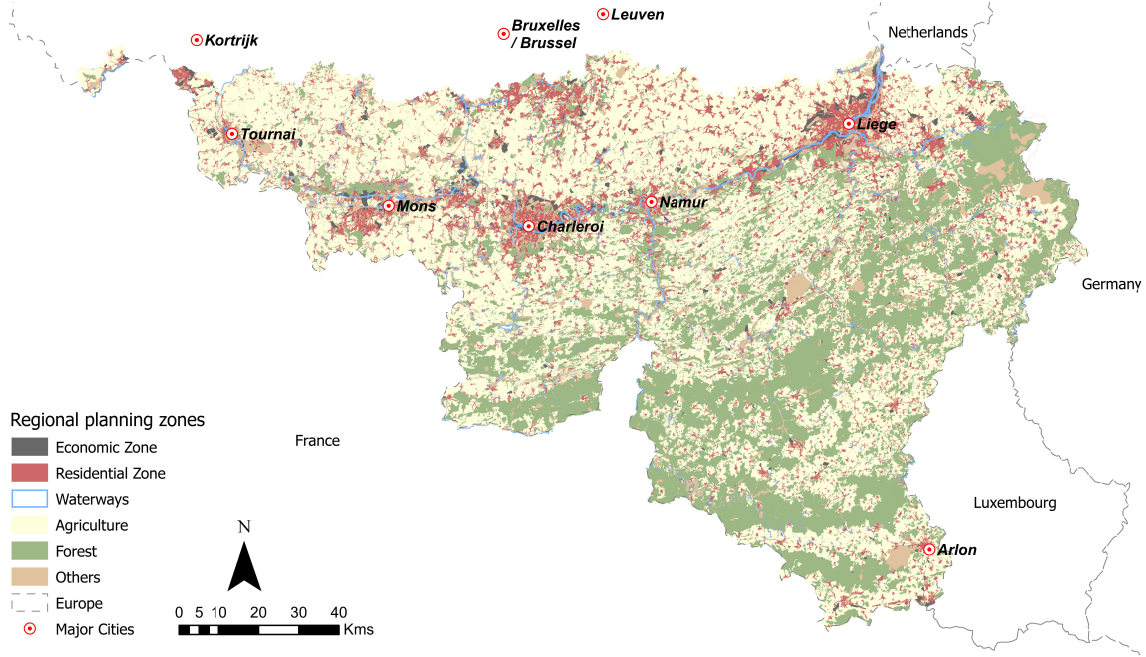


Figure 2: Study Area showing sector plan of Wallonia classified according to the intended use, source: [Public service of Wallonia \(2020\)](#)

Over time, more strategic and flexible planning strategies were adapted to balance urban expansion with environmental preservation ([Broitman and Koomen \(2015\)](#), [CPDT \(2024\)](#)). Despite these efforts, local governance remains crucial where municipalities have significant power over development decisions. This decentralised system ([Chakraborty et al. \(2025\)](#)) has created spatial disparities where urban expansion continues at varying rates across the region. Wallonia’s ongoing transformation highlights the challenges of managing land resources amidst such socio-economic pressures, making it an interesting case study for long-term urbanisation trends and planning strategies.

## 2.2 Datasets

Our methodology, as shown in [Figure 1](#), is designed to align with the available data – a crucial component of the model. Akin to the studies done by [Chakraborty et al. \(2022a\)](#) and [Chakraborty et al. \(2023\)](#), cadastral Data from the Belgian Land registry has been used as the dependent variable for mapping the urban built-up in Wallonia. We have used the attribute of ‘construction year’ to further create Built-up rasters for the years 2000, 2010, and 2020 at a scale of  $100\text{m} \times 100\text{m}$  corresponding to 1 hectare (ha). This is a commonly used scale for urban modelling studies like [Mustafa et al. \(2018a\)](#) and [Chakraborty et al. \(2024a\)](#). Several studies ([Cammerer et al. \(2013\)](#), [Tang et al. \(2005\)](#), [Beckers et al. \(2013\)](#)) consider urban growth as a binary method that fails to adequately exhibit the properties of urban built-up development at different levels of density. Hence, in our study, we classified rasters into four built-up density classes using geometric classification techniques ([Arlinghaus and Kerski \(2013\)](#)). The four density levels include *class 0–Non* built-up, *class 1–Low density* built-up, *class 2–Medium density* built-up, and *class 3–High density* built-up. This follows the method of dataset construction

based on the work done by [Chakraborty et al. \(2022a\)](#) and [Chakraborty et al. \(2024b\)](#). These maps are used for calculating land demand rates of historical built-up which are then used for simulating urban growth for the years 2030, 2040 and 2050. On the other hand, we selected a list of *twelve* independent variables comprising geophysical, accessibility, and socio-economic factors as shown in [Table 1](#). These variables have a direct impact in understanding urban growth dynamics as found in similar studies like ([Mustafa et al. \(2018a\)](#)), [Mustafa et al. \(2018c\)](#), [Mustafa et al. \(2018d\)](#)). We have used the Open Street Maps (OSM) ([OpenStreetMap Foundation contributors \(2024\)](#)) to define road type using the data attributes and calculated the Euclidean distance from them. The road types *Motorways* and *Highways* are defined as Road 1. Similarly, roads 2, 3, and 4 represent primary roads, secondary roads, and residential roads, respectively. Similarly, we acquired railway stations as point data from OSM. The slope has been calculated from the Digital Elevation Model derived from the Geoportal website of Wallonia by [Public service of Wallonia \(2020\)](#). The total population and the number of jobs, represented as the employment rate, have been considered socio-economic variables. While the former was derived at the statistical sector level, the latter was calculated at the municipal level, based on data from the Belgian statistical office (Statbel, [Statbel \(2017\)](#)). Statbel accounts for statistical figures about social, economic, and territorial sectors. One of the most important variables in our study includes zoning maps. Zoning has been proven to be an extremely significant variable for studying urban planning in Belgium. Belgium’s sector plan or *Plan de secteur*, as called in Wallonia, provides information about zones and their designated uses as shown in [Figure 2](#). It has been observed in multiple studies ([Poelmans and Van Rompaey \(2010\)](#), [Mustafa et al. \(2018d\)](#), [Chakraborty et al. \(2022a\)](#)) that zoning has played a crucial role in determining the urban development processes over the years. Hence, we created a binary zoning map where 0 means cells that are not permitted for urban development and 1 is permitted for further development.

Table 1: List of data used for modelling urban growth scenarios, source: Cadastral Data, FPS Belgium

| Name                            | Abbreviation | Initial Data Type   | Final Data Type | Unit        |
|---------------------------------|--------------|---------------------|-----------------|-------------|
| Elevation                       | DEM          | Raster              | Raster          | meter (m)   |
| Slope                           | SL           | Raster              | Raster          | percent (%) |
| Distance to Road 1              | ER1          | Vector <sup>a</sup> | Raster          | meter (m)   |
| Distance to Road 2              | ER2          | Vector <sup>a</sup> | Raster          | meter (m)   |
| Distance to Road 3              | ER3          | Vector <sup>a</sup> | Raster          | meter (m)   |
| Distance to Road 4              | ER4          | Vector <sup>a</sup> | Raster          | meter (m)   |
| Distance to Railway Stations    | ERS          | Vector <sup>b</sup> | Raster          | meter (m)   |
| Distance to Large Sized Cities  | ELC          | Vector <sup>b</sup> | Raster          | meter (m)   |
| Distance to Medium Sized Cities | EMC          | Vector <sup>b</sup> | Raster          | meter (m)   |
| Employment Density              | EMD          | Vector <sup>c</sup> | Raster          | per inh     |
| Population                      | POP          | Vector <sup>c</sup> | Raster          | numeric     |
| Zoning                          | ZON          | Vector <sup>c</sup> | Raster          | meter (m)   |

Vector data type that has been used for pre-processing: <sup>a</sup>Line, <sup>b</sup>Point, <sup>c</sup>Polygon  
All the data have been resampled to 100m × 100m and standardized before running the modelled scenarios

Prior to modelling, all the independent variables have been standardised using the z-score normalisation technique to use in our model, ensuring comparability of the output. Additionally,

Table 2: Class to class transition of urban built-up demand (with percentages).

| Years     |         | Class 0   | Class 1        | Class 2        | Class 3        |
|-----------|---------|-----------|----------------|----------------|----------------|
| 2000–2010 | Class 0 | 1,391,031 | *7169 (27.60%) | *5247 (20.20%) | *1271 (4.89%)  |
|           | Class 1 |           | 70,983         | †7920 (30.50%) | †248 (0.95%)   |
|           | Class 2 |           |                | 149,554        | †4115 (15.85%) |
|           | Class 3 |           |                |                | 52,582         |
| 2010–2020 | Class 0 | 1,381,843 | *4906 (26.28%) | *3538 (18.95%) | *744 (3.99%)   |
|           | Class 1 |           | 72,337         | †5613 (30.07%) | †202 (1.08%)   |
|           | Class 2 |           |                | 159,056        | †3665 (19.63%) |
|           | Class 3 |           |                |                | 58,216         |

\* Expansion, † Densification

we have ensured that no collinearity exists between the independent variables. Hence, we have calculated the Variation Inflation Factor (VIF) for each variable, considering all the variables with VIF values  $< 4$ , similar to [Khuri \(2013\)](#) and [C. Montgomery et al. \(2012\)](#).

### 2.3 Demand calculation

In this paper, we attempt to model the future urban growth scenarios by extrapolating their past demand under two different demand conditions. *Demand* refers to the development of new built-up cells observed between two time-stamps  $T1$  and  $T2$  as shown in [Figure 1](#). While this demand can be expressed in terms of per day or year, our study performs a long-term assessment considering two decades: 2000-2010 and 2010-2020, as presented in [Table 2](#) to simulate future growth until 2050.

As mentioned in section [Introduction](#), we have calculated demand for urban growth under BAU and GAU demand scenarios to understand their effect on land take. In [Table 2](#), we present the class-to-class transition matrix for urban built-up for the years 2000-2010, and 2010-2020, which we will use to further calculate the demand for the following years, to model the change in built-up. The transitions from reference class 0 to classes 1, 2, and 3 are considered as urban expansion, and transitions from class 1 to 2 and 3, and class 2 to 3, are considered urban densification.

The demand simulation in the case of BAU is calculated according to [Equation 1](#). It is the mathematical formulation for extrapolating demand for any particular class transition, for the BAU scenario. This is accomplished using the demand data of two previous years.

$$d = \frac{D_n - D_m}{n - m}, \quad n > m \quad (1a)$$

$$D_x = D_n + (x - n) \times d, \quad (1b)$$

where  $x \in \mathbb{Z}$ ,  $D_x \geq 0$

where  $D_x$  is the yearly demand at year  $x$  and  $d$  is the change rate used to extrapolate the demand for the simulation.

[Equation 1a](#) calculates the change in demand between two years  $m$  and  $n$ , over the duration  $n - m$  years. Demand at any year  $x$  is assumed to be constant throughout that particular year. For the subsequent year, the demand is recalculated. Thus, we obtain the yearly "rate" of change  $d$ , assuming that the change is linear. [Equation 1b](#) explains how this change rate  $d$  can then be used to extrapolate over the following years to predict 2030, 2040 and 2050. This yearly demand, hence calculated, is used for modelling the allocation of class transitions.

We use an example to illustrate [Equation 1](#) further. We observe from the [Table 2](#) that there is a demand of 7169 cells from class 0 to 1 for the years 2000-2010. We first calculate the change rate (using [Equation 1a](#)) rate to be

$$d = \frac{D_{2020} - D_{2010}}{2020 - 2010} = \frac{490.6 - 716.9 \text{ (hectare/year)}}{2020 - 2010 \text{ (years)}} = -22.63 \text{ ha/year}^2$$

A decline in yearly demand for any class transition is hence characterised by a negative change rate. Similarly, we have calculated the demand for the remaining class transitions of reference class 0 to 2 and 3, reference class 1 to 2 and 3, and reference class 2 to 3. The change rate is now used to calculate the demand for any year after  $n$  (after 2020, in our case). Using [Equation 1b](#), we get, for instance, the demand in the year 2030 to be

$$\begin{aligned} D_{2030} &= D_{2020} + (2030 - 2020) \times d = 490.6 + 10 \times (-22.63) \\ &= 264.3 \text{ ha/year or } 0.72 \text{ ha/day} \end{aligned}$$

We thus see the demand for urban expansion decrease over time.

Coming to the case of GAU, we assume a constant demand for every year after year  $n$  (2020, in our case), and hence the change rate  $d$  to be 0. The demand in the year 2030 and the subsequent years, for the GAU case, from class 0 to 1 transition would hence be

$$D_{2030} = D_{2020} = 490.6 \text{ ha/year or } 1.34 \text{ ha/day}$$

which is higher than the value in the BAU scenario. Similarly, in both cases, demands are calculated for the remaining class transitions. This example, thus, clearly demonstrates how the trend varies in each case – a linear extrapolation in the BAU scenario while being a constant demand in the GAU scenario as further discussed in section [Results](#).

## 2.4 Cellular Automata modelling for futuristic scenario simulation

Urban development involves changes in built-up areas, where previously unutilized land transitions into spaces such as residential, commercial, or industrial zones—a process termed urban expansion. This occurs as occupied land extends into areas that were once greenfields. Conversely, areas already in use may undergo densification, where existing urban zones are further developed to accommodate growing populations, increasing the population density. To model and analyse these different forms of urban development, Cellular Automata (CA) modelling has been widely used ([Batty \(1997\)](#), [Li and Yeh \(2000\)](#)) because of its dynamic and temporally explicit nature. CA represents urban areas as grids of cells evolving based on transition rules.

In this study, we allocate the demand (as explained in sub-section [Demand calculation](#)) for future urban expansion and densification under BAU and GAU scenarios in 2030, 2040 and 2050.

The transition rule is defined based on two components :

- Probability maps derived by Multinomial Logistic regression (MNL) model.
- Neighbourhood calibration using CA Model.

#### 2.4.1 Model Calibration and Probability Maps

Several studies ([Clarke et al. \(1996\)](#), [Silva and Clarke \(2002\)](#), [Waddell \(2002\)](#)) elucidate the importance of calibration in modelling, for near-realistic simulation. In this study, we employ an MNL to calibrate our dependent variable (e.g. built-up changes) based on various independent variables as shown in [Table 1](#). It analyses changes for class 0 (no-change/transition to class 1, 2, or 3), class 1 (no-change/transition to class 2), and class 2 (no-change/transition to class 3). Similar to the studies by [Mustafa et al. \(2018b\)](#) and [Chakraborty et al. \(2022b\)](#), we divided our data into a 70-30 ratio of training and testing sets. The training set comprises 24034 randomly sampled cells (the 70%), ensuring minimal autocorrelation for the years 2000-2010. This is an efficient way to handle autocorrelation ([Overmars et al. \(2003\)](#)) in our dependent variables, i.e., urban built-up maps ([Cammerer et al. \(2013\)](#), [Rienow and Goetzke \(2015\)](#)).

The suitability maps are obtained for each class by the following equation

$$\begin{aligned} \log(k_1) &= \alpha_{k_1} + \beta_{k_1\text{DEM}}(\text{DEM}) + \beta_{k_1\text{SL}}(\text{SL}) + \cdots + \beta_{k_1\text{ZON}}(\text{ZON}) \\ &\vdots \\ \log(k_n) &= \alpha_{k_n} + \beta_{k_n\text{DEM}}(\text{DEM}) + \beta_{k_n\text{SL}}(\text{SL}) + \cdots + \beta_{k_n\text{ZON}}(\text{ZON}) \end{aligned} \quad (2)$$

The MNL model provides a set of coefficients used to compute probability maps for determining the likelihood of new urban cell growth. It also shows the important variables having a positive or negative impact on urban growth. Alongside, we also computed significant variables with  $p\text{-value} < 0.01$ . These maps are then used as input for defining transition rules and spatial allocation of future urban growth demand.

#### 2.4.2 Neighbourhood effect on demand allocation

The probability alone does not consider the local effect of urban built-up. Hence, we use the CA model to calibrate the neighbourhood effect on urban growth. To do so, we use a  $3 \times 3$  grid of cells – also known as Moore’s neighbourhood. This particular window size has been chosen as many studies ([White and Engelen \(2000\)](#), [Poelmans and Van Rompaey \(2009\)](#), [Zaitsev \(2017\)](#)) have proved it to be efficiently capturing urban growth phenomena because of its easy configuration and sufficient local characteristics ([Zhang and Wang \(2021\)](#)). The neighbourhood for a given cell is calculated as given below.

$$N_{ij}^{c_1, c_2} = \sum_{n=j-1}^{j+1} \sum_{m=i-1}^{i+1} \delta(c_{mn}, c_2) \cdot (1 - \delta_{m,i} \cdot \delta_{n,j}) \quad (3a)$$

$$\text{where } \delta_{a,b} = \begin{cases} 1, & \text{if } a = b, \\ 0, & \text{otherwise.} \end{cases} \quad (3b)$$

where  $N_{ij}^{c_1, c_2}$  is the  $3 \times 3$  Moore's neighbourhood for the cell at index  $(i, j)$ . The cell is to transition from class  $c_1$  to class  $c_2$ . Here,  $N_{ij}^{c_1, c_2}$  is defined as the number of cells in the neighbourhood of cell  $(i, j)$  that have the class  $c_2$ . Equation 3a calculates the neighbourhood by comparing the class of each cell in the neighbourhood ( $c_{mn}$ ) with  $c_2$ .  $\delta_{a,b}$  here is the Kronecker delta function, defined in Equation 3b.

Consolidating the effects of both – the probability maps from MNL ( $P_{ij}^{c_1, c_2}$ ) and the neighbourhood interactions ( $N_{ij}^{c_1, c_2}$ ) as described above, we define the transition potential ( $T_{ij}^{c_1, c_2}$ ) – the realistic likelihood of a cell  $(i, j)$  transitioning from class  $c_1$  to  $c_2$ , below, in Equation 4a. Following this, we form the transition rule, which is a mathematical formulation for the spatial allocation of the potent cells at every time step. It makes the backbone of our MNL-CA model. To incorporate a degree of randomness while preserving the transition potential as the primary determinant, transitions are permitted only when their potential exceeds a randomly generated value drawn from a Gaussian distribution constrained between 0 and 1 (Equation 4b).

$$T_{ij}^{c_1, c_2} = \sqrt{P_{ij}^{c_1, c_2} \times N_{ij}^{c_1, c_2}} \quad (4a)$$

$$T_{ij}^{c_1, c_2} > n, \quad n \in U([0, 1]) \quad (4b)$$

Considering the CA transition rule and the above-mentioned methods, we cumulatively allocate new built-up cells for each year (time step  $T_n$ ), giving us the simulated built-up map comprising all class transitions. As a part of our modelling, we first simulate a map of 2020 (based on 2000-2010 demand) to compare it with the observed map for the same year.

### 2.4.3 Validation of the Model

Once we simulate the map for 2020, we validated it with observed 2020 urban built-up maps before further simulation. Validation helps to understand the robustness of a model's ability to predict accurately. In our study, we have used two well-known metrics for validating our model's output. They are:

1. **The Relative Operating Characteristics (ROC) curve** evaluates the goodness of fit in MNL models by comparing a probability map with actual outcomes (Hu and Lo (2007)). The key component of ROC analysis is the Area Under the Curve (AUC), which measures the model's ability to distinguish between classes, with values ranging from 1.0 (perfect) to 0.5 (no discriminative power) (Pontius and Schneider (2001)). One of the significant advantages of the ROC method is its independence from class distribution, allowing fair comparisons across different models or scenarios. In urban growth studies, it is useful for assessing models like CA and machine learning approaches, where spatial transitions are key (Chen et al. (2014)). The ROC curve plots True Positive Rate (TPR) vs. False Positive Rate (FPR), demonstrating the trade-off between sensitivity and specificity. This versatility underscores its relevance in validating urban growth simulations and planning frameworks.

The AUC is calculated as

$$AUC = \int_0^1 TPR(x) dx \quad (5)$$

where **AUC** represents the Area Under the Curve, a summary statistic used to evaluate model performance.  $TPR(x)$  is the True Positive Rate (TPR) as a function of the threshold  $x$ , and  $dx$  represents the infinitesimal change in the False Positive Rate (FPR). The TPR and FPR are calculated using the following equations.

$$TPR = \frac{True\ Positives}{True\ Positives + False\ Negatives} \quad (6a)$$

$$FPR = \frac{False\ Positives}{False\ Positives + True\ Negatives} \quad (6b)$$

where TPR shows the proportion of actual positives (urban transitions) that are correctly identified by the model. FPR represents the proportion of negatives (non-urban parcels) incorrectly identified as positives.

2. **Kappa Statistics (Cohen's Kappa,  $\kappa$ )** assesses the agreement between two categorical variables in classification tasks. In urban growth modelling,  $\kappa$  compares predicted and observed land cover to evaluate model accuracy (Congalton (1991)). Unlike ROC,  $\kappa$  values range from -1 to 1, where 1 indicates perfect agreement, 0 represents random chance, and negative values suggest less agreement than expected by chance (Rwanga et al. (2017)).  $\kappa$  accounts for chance agreement, making it a more robust measure than simple accuracy. It is commonly used in urban growth models, such as CA and machine learning, to ensure reliable simulations that reflect real-world patterns (Li and Yeh (2000)). In dynamic urban environments,  $\kappa$  helps evaluate the accuracy of land-use change models (Wang et al. (2012)).

The general formula of Cohen's Kappa is expressed as given below.

$$\kappa = \frac{P_o - P_e}{1 - P_e} \quad (7)$$

where  $P_o$  is the observed agreement (accuracy) and  $P_e$  is the expected agreement by chance. The interpretation is as follows:

- $\kappa = 1$ : perfect agreement
- $\kappa = 0$ : agreement is no better than chance
- $\kappa < 0$ : worse than chance.

Once an accurate validation between observed and simulated maps is observed, we simulate future predictions for years 2030, 2040 and 2050 for BAU and GAU scenarios to evaluate the spatial distribution affecting land-take under the two different demand scenarios.

## 2.5 Spatial metrics as a measure of land-take

Spatial metrics are quantitative tools used in urban modelling to analyse and represent spatial structures and patterns. This will improve the understanding of the land-take scenario and will

guide towards sustainable development by analysing urban structure and composition. To align with our aim of simulating urban growth and understanding land-take scenarios in Wallonia, it is important to assess growth patterns and their distribution types. Hence, we developed a Python workflow to compute spatial metrics determining the kind of urban growth primarily governing the land-take in our study area for both the growth scenarios.

Wallonia has a dominance in rural development with some important urban cores like Liege, Mons, Namur, etc. (Figure 2). This is why we use spatial metrics as a tool to understand the development pattern, especially in the context of land consumption. While most studies deal with the amount of land-take or area consumed by urban growth, there are few works done for understanding the spatial pattern governing them (Martin et al. (2005), Hosseinali et al. (2013), Colsaet et al. (2018)). In our study, we extend the simulation of the land take scenario by supporting it with its spatial pattern. Below, in Table 3, are the selected spatial metrics used in our study to understand the landscape pattern under growth scenarios.

Table 3: Description of selected metrics used in urban growth analysis.

| Metric                   | Formula   | Explanation   |
|--------------------------|---|---|
| Urban Sprawl Index (USI) | $USI = \frac{\text{Built-up area}}{\text{Urban extent}}$                  | Measures the extent of sprawl by assessing the ratio of built-up area to urban extent.  |
| Shannon Entropy (SE)     | $H = - \sum_{i=1}^n p_i \ln(p_i)$   | Quantifies urban distribution uniformity; higher values indicate more dispersed growth. |
| Patch Density (PD)       | $PD = \frac{\text{Number of patches}}{\text{Total area}}$                 | Describes fragmentation; higher values signify more fragmented urban landscapes.        |
| Average Contiguity (AC)  | $AC = \frac{\sum \text{Contiguity of patches}}{\text{Number of patches}}$ | Indicates urban compactness; higher values suggest more contiguous growth.              |

## 3 Results

### 3.1 Impact of independent variables on urban growth

We calibrated our MNL model for urban expansion (reference class 0 to built-up classes 1, 2 and 3), and urban densification (reference class 1 to 2 and 3, and reference class 2 to 3). The model produces coefficients for each independent variable, showing their respective contribution to the process of urban expansion and densification.

Our findings, depicted in Figure 3, show that *zoning* policies emerge as the most significant explanatory variable having a positive impact on the **urban expansion** process with coefficient value of 3.450, 3.035 and 3.374. This observation is in line with Mustafa et al. (2018b) and Poelmans and Van Rompaey (2010). As for the geophysical factors, *Elevation* has an overall positive impact on the development of low-density cells (coefficient of 0.042) while having a negative impact on high-density built-up development. *Slope*, on the other hand, has a negative impact across all three built-up classes. Overall, we observe that distance to roadways has a negative impact on the urban expansion processes (*Highways*) in Table 1. Distance to railway stations (*ERS*) has no significant impact on low and medium built-up density and a negative

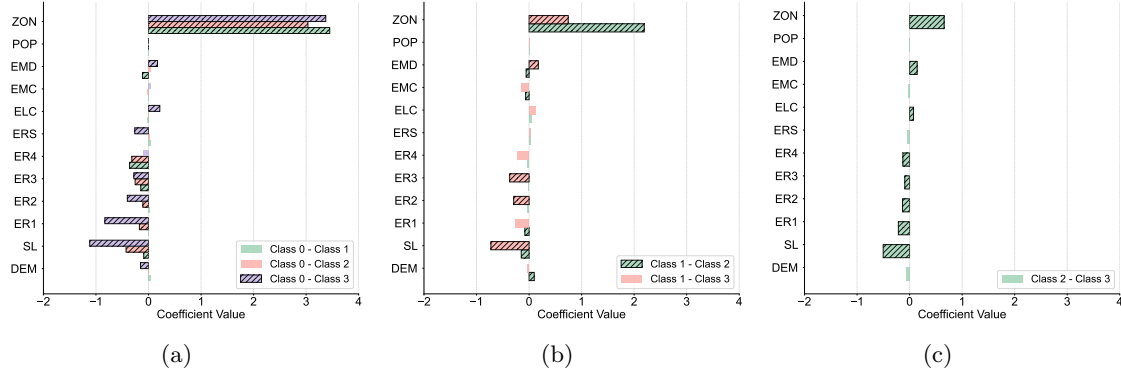


Figure 3: Graphs showing coefficients derived from MNL model for (a) urban expansion (reference class 0), (b) urban densification (reference class 1) and (c) urban densification (reference class 2).

(Hatched bar shows variables significant at  $p$ -value  $< 0.01$ )

impact on high density expansion, i.e. cells located further away from the stations have a lower chance of being urbanised with high density cells. The variables *ELC* and *EMC* (Table 1) have a positive impact with values 0.001 and 0.216, on high-density expansion. On the contrary, it has a negative impact, particularly in low-density expansion. *EMD* or job density measures the number of jobs available in different categories per municipality area. For higher density built-up, it has a positive impact while it reflects a negative impact in low density built-up expansion, even though significant.

While calibrating **urban densification** using MNL, similar to expansion zoning, has been a significant positive variable impacting the urban densification process. Elevation derived from DEM and slope largely affect the process with an increase in density levels. However, the negative coefficient has significance in terms of its  $p$ -value. Pertinent to our observation regarding accessibility, the densification process is also negatively impacted by distance to *roads* even though their significance prevails in medium and high built-up classes. Similar to expansion, *ERS* (Table 1), on the other hand, reflects a positive coefficient of 0.027 and 0.031 (class 1 to 2 and 3), and negative in medium to high density class transition. However, the impact of railway station does not hold a significant relationship. Distance to Large cities holds a non-significant impact on medium and high-density built-up, while medium cities negatively impact urban densification. The density of jobs attracts more built-up development, thus found to have significance with positive coefficients (0.177 and 0.144) for medium and high density built-up, respectively.

The ability of an MNL model's calibration can be measured using a probability map showing the likelihood of built-up occurrence to a binary map of actual occurrence. This probability map results from the coefficient produced by MNL. ROC value is a robust and widely used technique which indicates that a value  $> 0.5$  indicates a model's good fit (Hu and Lo (2007), Wang et al. (2012)). In our study, we computed the ROC for urban expansion (class 0 to 1, 2 and 3) based on the probability map and observed built-up maps. The values are 0.790, 0.840 and 0.930 for class 1, 2 and 3, respectively. Similarly, ROC for densification also suggested high calibration ability of MNL as shown in Table 4.

Table 4: ROC value of MNL model for each density class transition (row to column).

|         | Class 1 | Class 2 | Class 3 |
|---------|---------|---------|---------|
| Class 0 | 0.790   | 0.840   | 0.930   |
| Class 1 | –       | 0.989   | 0.991   |
| Class 2 | –       | –       | 0.978   |

### 3.2 Accuracy assessment for MNL-CA growth modelling

The model accounts for transitions both from non-built-up to built-up density classes and from lower to higher built-up density classes. To assess its predictive performance in allocating built-up demand, we simulated the built-up map for the year 2020 based on demand data from 2000–2010. This simulated map was then compared with the observed 2020 built-up map, derived from Belgium’s cadastral data, to evaluate the model’s accuracy.

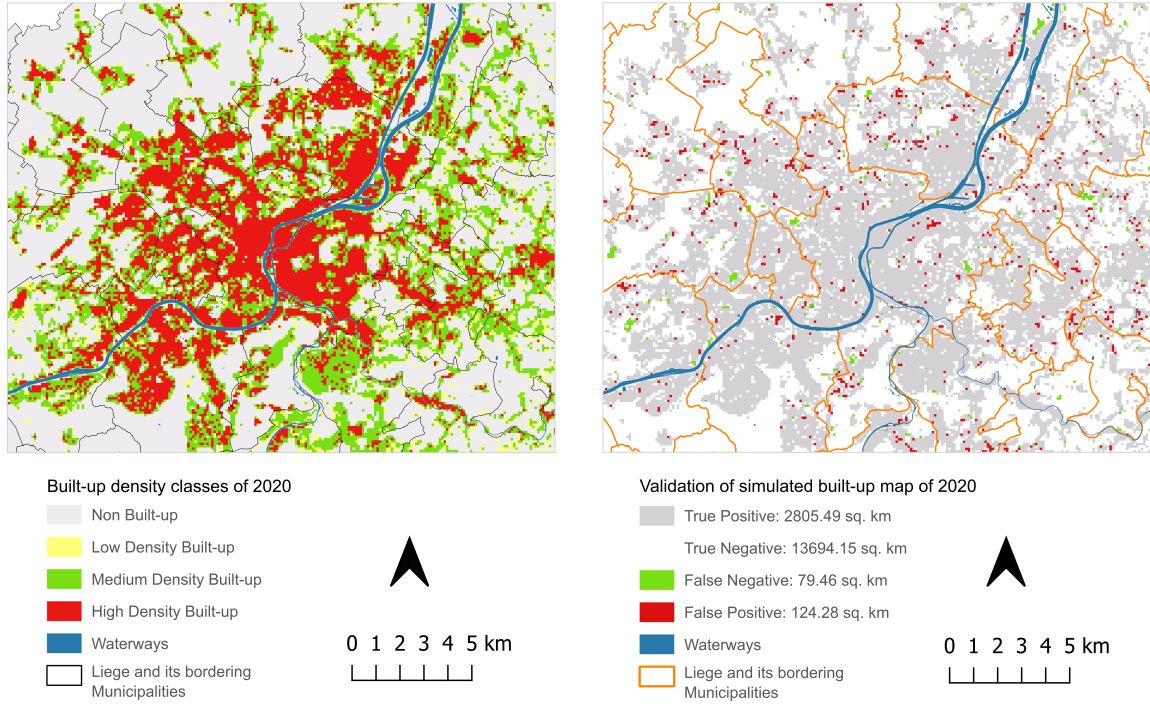
Figure 4(a) shows the built-up map, depicting the 4 density classes for the year of 2020. Understanding this spatial distribution is crucial for assessing the model’s performance. The model achieved high ROC values across built-up density classes: 0.994 (class 0), 0.923 (class 1), 0.963 (class 2), and 0.965 (class 3). The overall Cohen’s Kappa ( $\kappa$ ) coefficient was 0.925, indicating substantial agreement between the observed and simulated maps. To further evaluate the reliability of these results, an accuracy map of the simulated result has been visually represented in Figure 4(b). By comparing it to the built-up map, spatial patterns of over- and under-predicted cells become evident, highlighting areas of alignment with observed data as well as regions with notable discrepancies.

It is usually noted that the calibration accuracy of a model tends to surpass its validation accuracy (Al-Ahmadi et al. (2009), García et al. (2012)). This limitation can be attributed to the simulation’s inability to account for the inherent uncertainty in the allocation of built-up areas observed in real-world scenarios. To address this, we incorporated a stochastic component into the CA model, which improved its ability to handle variability and achieve realistic simulations.

### 3.3 Simulation of future urban development under the BAU and GAU scenarios

The urban growth simulation until 2050 under the BAU and GAU scenarios offers a comprehensive comparison of land-use planning in Wallonia. Using the MNL-CA model, the demand derived for both scenarios was allocated, enabling an analysis of the temporal changes in urban growth. Previous studies, such as Mustafa et al. (2018a) and Thorne et al. (2013), have employed BAU growth approaches for futuristic predictions, by linearly extrapolating the past demand over multiple years to simulate future scenarios. Similar to their findings, we identified a progressive shift from expansion to densification in Wallonia between 2000-2020 (Table 2). Even then, the expansion processes remained predominant. Alongside this, our study makes an assumption of *Growth-As-Usual*, the most recent observed demand extrapolated constantly to make projections about the future.

The BAU scenario, which extrapolates historical demand, shows a steady decrease in land take over time. Starting at 1.79 hectares/day in 2020, the daily land take gradually reduces



(a) Zoomed image of Liège municipality showing built-up density classes for the year 2020 (b) Accuracy map, showing pixel-level comparison of urban growth model between observed and simulated map of 2020.

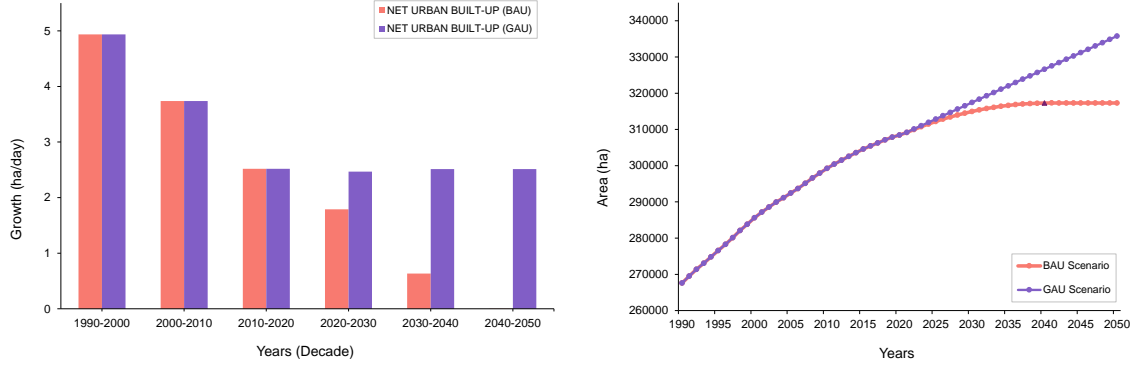
Figure 4: Built-up and accuracy map of Liège and its surroundings, for the year 2020.

to 0 hectares/day by 2040 itself, indicating a complete stabilisation in demand for new urban land. This stabilisation serves as an *inflection point* for expansion demand and is reflected in Figure 5(a), where the BAU curve flattens after 2040. Our study reveals a decline in demand for expansion (from class 0 to classes 1, 2, and 3) and a corresponding rise in demand for densification (Table 5), aligning with these trends. The total built-up area under BAU increases by 8861 hectares between 2020 and 2050, corresponding to a growth of 2.87%. In contrast, the GAU scenario assumes a constant land take rate of 2.51 hectares/day throughout the simulation period, leading to a significantly higher cumulative increase in built-up area. By 2050, the GAU scenario adds 27347 hectares, resulting in a total growth of 8.87%.

The net built-up area over time is depicted in Figure 5(b), highlighting the contrasting trajectories of the two scenarios. The BAU scenario demonstrates a tapering growth rate after 2020, with stabilisation occurring by 2040. Meanwhile, the GAU scenario maintains a linear growth pattern, maintaining a consistent positive slope even at 2050.

As presented in Table 5, the demand for class-to-class transitions across both scenarios from 2020 to 2050 illustrates distinct trends. In the BAU scenario, the rate of decline in the demand for expansion exceeds that of densification, leading to higher expansion until 2020, after which densification becomes the prevailing trend.

Class-wise transitions highlighting the divergence between the BAU and GAU scenarios are shown in Figure 6. In contrast to the BAU scenario, which reflects a notable decline in the percentage of demand for outward expansion over time, the GAU scenario sustains a steady



(a) Plot of simulated demand, depicting the divergence in the BAU and GAU scenarios. (b) Plot of area occupied by urban land, as a function of time.

Figure 5: Comparison of land use and urban growth in the BAU and GAU scenarios.

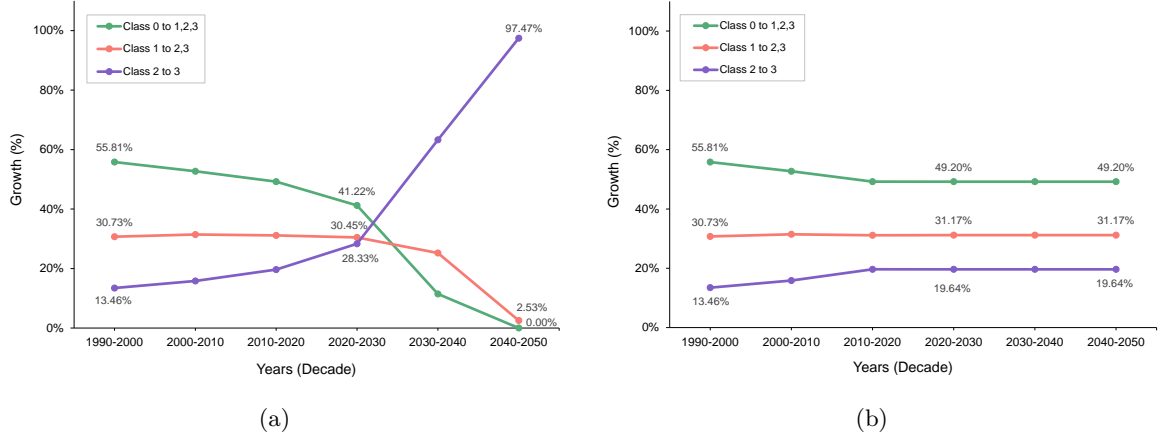


Figure 6: Decade-wise percentage of expansion and densification for (a) BAU scenario and (b) GAU scenario.

percentage of demand for expansion (Table 6). This divergence is evident in class 1 (low-density urban land), which consistently declines, shrinking by 2286 hectares (-2.94%) under BAU and 3166 hectares (-4.08%) under GAU. Meanwhile, class 2 (medium-density urban land) grows modestly by 1271 hectares (+0.76%) under BAU but expands substantially by 16590 hectares (+9.87%) under GAU, highlighting its increasing role in urban growth. Class 3 (high-density urban land) shows changes, with a 15.75% increase under BAU and a 22.20% rise under GAU.

Table 7 presents the quantified changes in spatial metrics across scenarios and years, highlighting distinct urban growth patterns. The *Urban Sprawl Index* (USI) increases from 0.658 in 2020 to 0.668 under the BAU scenario and 0.697 under the GAU scenario by 2050, indicating a higher degree of sprawl in the GAU scenario. Similarly, *Shannon Entropy* (SE) rises from 0.950 in 2020 to 0.957 under BAU and 0.976 under GAU, reflecting greater spatial heterogeneity under the latter. Class-wise *Average Contiguity* (AC) shows a notable increase, particularly in classes 2 and 3, with values reaching 3.936 and 5.248 under BAU and 5.760 and 5.810 under GAU, by 2050. *Patch Density* (PD) decreases over time for all classes, with lower values observed in GAU compared to BAU in 2050, indicating fewer but larger urban patches in the

Table 5: Class-to-class demand for simulated urban built-up of 2030–2050 under the BAU and GAU scenarios.

| Years     |         | BAU     |         |         |         | GAU     |         |         |         |
|-----------|---------|---------|---------|---------|---------|---------|---------|---------|---------|
|           |         | Class 0 | Class 1 | Class 2 | Class 3 | Class 0 | Class 1 | Class 2 | Class 3 |
| 2020–2030 | Class 0 | 1377173 | 2640    | 1820    | 210     | 1372673 | 4900    | 3530    | 740     |
|           | Class 1 |         | 73793   | 3300    | 150     |         | 71433   | 5610    | 200     |
|           | Class 2 |         |         | 164997  | 3210    |         |         | 164547  | 3660    |
|           | Class 3 |         |         |         | 62827   |         |         |         | 62827   |
| 2030–2040 | Class 0 | 1376673 | 380     | 120     | 0       | 1363503 | 4900    | 3530    | 740     |
|           | Class 1 |         | 75333   | 990     | 110     |         | 70523   | 5610    | 200     |
|           | Class 2 |         |         | 167357  | 2760    |         |         | 170027  | 3660    |
|           | Class 3 |         |         |         | 66397   |         |         |         | 67427   |
| 2040–2050 | Class 0 | 1376673 | 0       | 0       | 0       | 1354333 | 4900    | 3530    | 740     |
|           | Class 1 |         | 75653   | 0       | 60      |         | 69613   | 5610    | 200     |
|           | Class 2 |         |         | 166157  | 2310    |         |         | 175507  | 3660    |
|           | Class 3 |         |         |         | 69267   |         |         |         | 72027   |

Table 6: Projected urban growth across density classes (2020–2050) under BAU and GAU scenarios

| Density Class | Area-2020 | BAU Scenario |        |            | GAU Scenario |        |            |
|---------------|-----------|--------------|--------|------------|--------------|--------|------------|
|               |           | Area-2050    | Change | Growth (%) | Area-2050    | Change | Growth (%) |
| Class 0       | 1381707   | 1372819      | -8888  | -0.64      | 1354333      | -27374 | -1.98      |
| Class 1       | 77679     | 75393        | -2286  | -2.94      | 74513        | -3166  | -4.08      |
| Class 2       | 168057    | 169328       | 1271   | 0.76       | 184647       | 16590  | 9.87       |
| Class 3       | 62704     | 72580        | 9876   | 15.75      | 76627        | 13923  | 22.20      |
| Overall       | 308440    | 317301       | 8861   | 2.87       | 335787       | 27347  | 8.87       |

former. These metrics collectively capture the differences in compactness, connectivity, and spatial arrangement of urban areas across the two scenarios.

Choropleth maps show the spatio-temporal distribution of built-up density across 262 municipalities in Wallonia (Figure 7). A geometric interval classification divides the values into five ranges, with darker colours indicating higher values (Figure 8 and Figure 9).

Under the BAU scenario (Figure 8), urban expansion from class 0 to 1, 2, and 3 remains limited, with growth concentrated primarily in urban centres (Figure 2) and its nearby suburban areas during the 2020–2030 period. By 2040–2050, expansion diminishes significantly. Densification, characterised by transitions from class 1 to class 2 and subsequently to class 3, is predominantly confined to urban cores, with minimal transformation occurring in rural and less urbanised municipalities in southern Wallonia. As we proceed to 2040–2050, even though expansion decreases, we can observe that the surrounding areas of the main urban centres continue to experience urban expansion, albeit at a slower pace. Conversely, the GAU scenario (Figure 9) projects more extensive and accelerated land-use changes, marked by geographically

Table 7: Table showing selected urban growth parameters for different scenarios and years.

| Year | Scenario | USI   | SE    | Class   | AC      | PD       |
|------|----------|-------|-------|---------|---------|----------|
| 2020 | -        | 0.658 | 0.950 | Class 0 | 382.987 | 1.81E-07 |
|      |          |       |       | Class 1 | 0.398   | 1.50E-06 |
|      |          |       |       | Class 2 | 3.394   | 1.16E-06 |
|      |          |       |       | Class 3 | 3.485   | 4.64E-07 |
| 2050 | BAU      | 0.668 | 0.957 | Class 0 | 538.398 | 1.29E-07 |
|      |          |       |       | Class 1 | 0.472   | 1.40E-06 |
|      |          |       |       | Class 2 | 3.936   | 1.05E-06 |
|      |          |       |       | Class 3 | 5.248   | 4.18E-07 |
| 2050 | GAU      | 0.697 | 0.976 | Class 0 | 632.839 | 1.08E-07 |
|      |          |       |       | Class 1 | 0.684   | 1.22E-06 |
|      |          |       |       | Class 2 | 5.760   | 9.01E-07 |
|      |          |       |       | Class 3 | 5.810   | 4.17E-07 |

dispersed expansion and pronounced densification beyond urban cores. Growth extends into peri-urban and rural areas, with notable intensification occurring in municipalities under population pressures and near economic hubs such as Charleroi, Liège, Namur, and the Brussels periphery (e.g., Wavre and Ottignies-Louvain-la-Neuve).

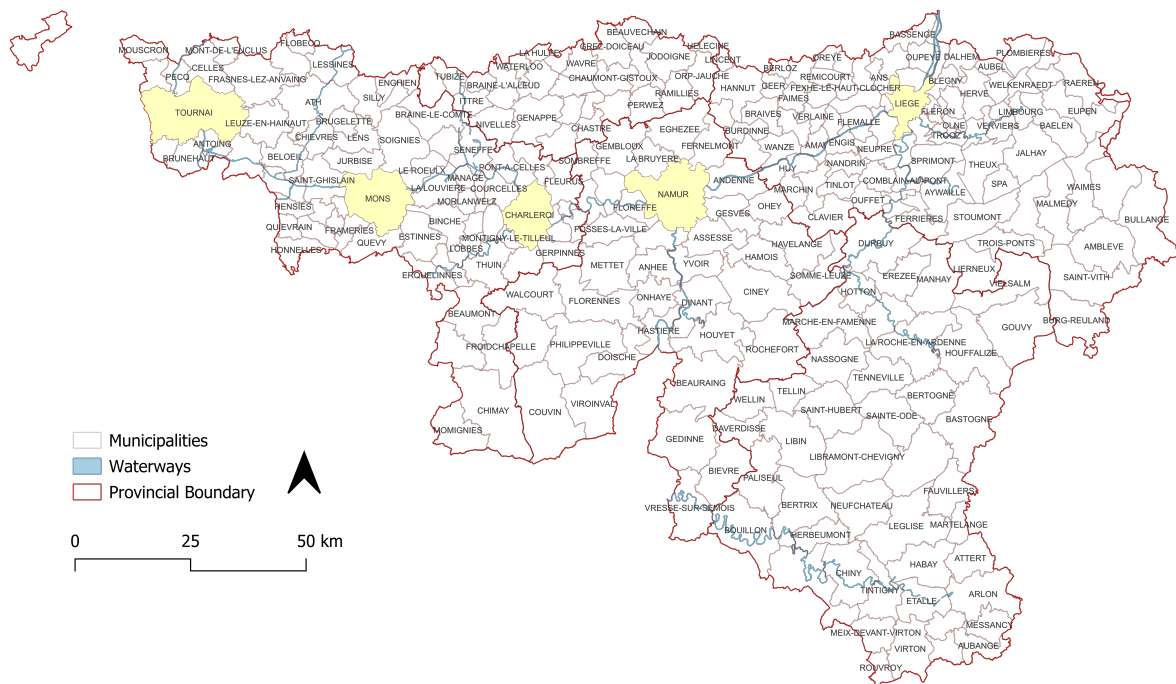


Figure 7: Municipalities of Wallonia

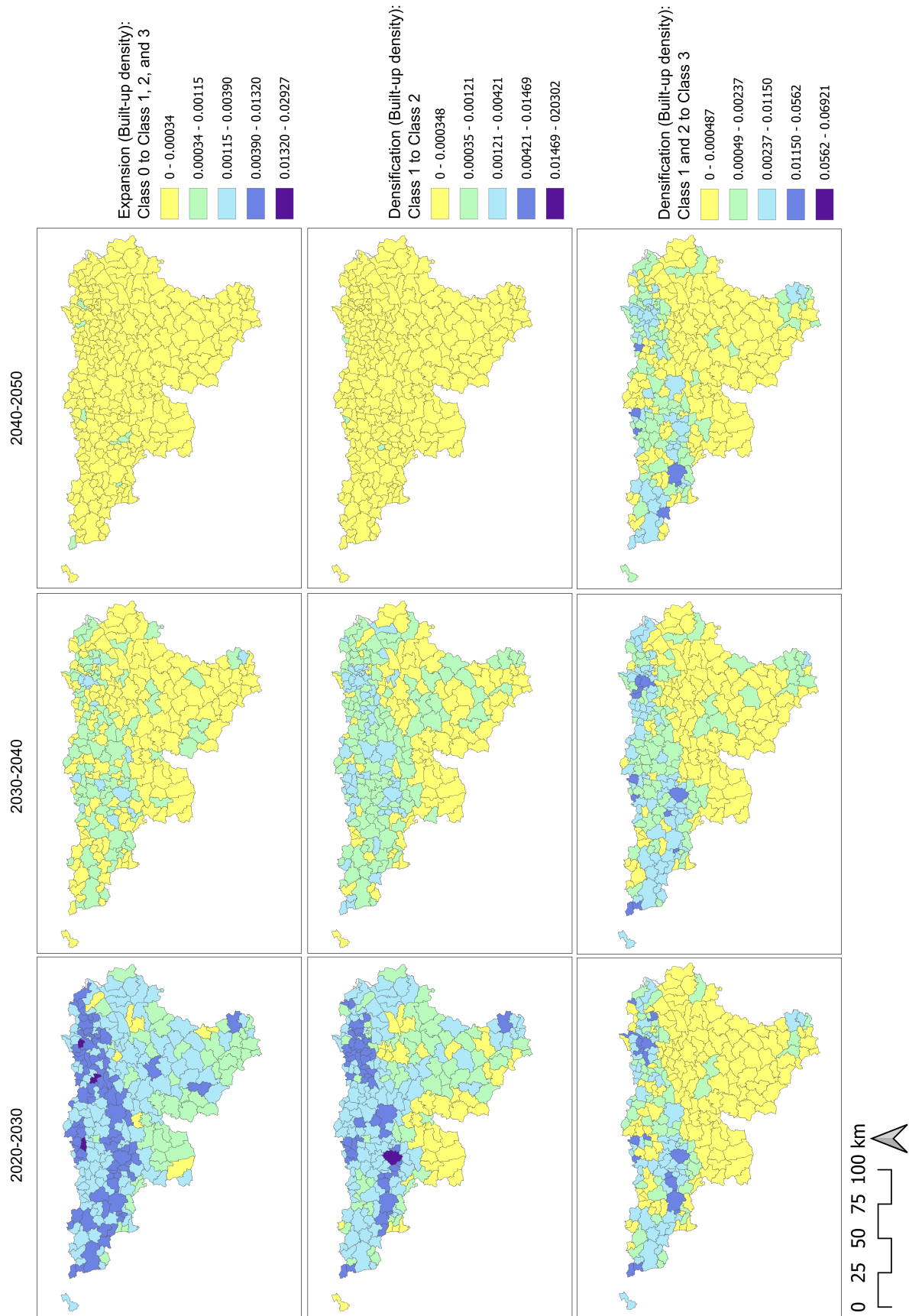


Figure 8: Choropleth map showing spatial distribution of built-up density per municipality for the BAU scenario

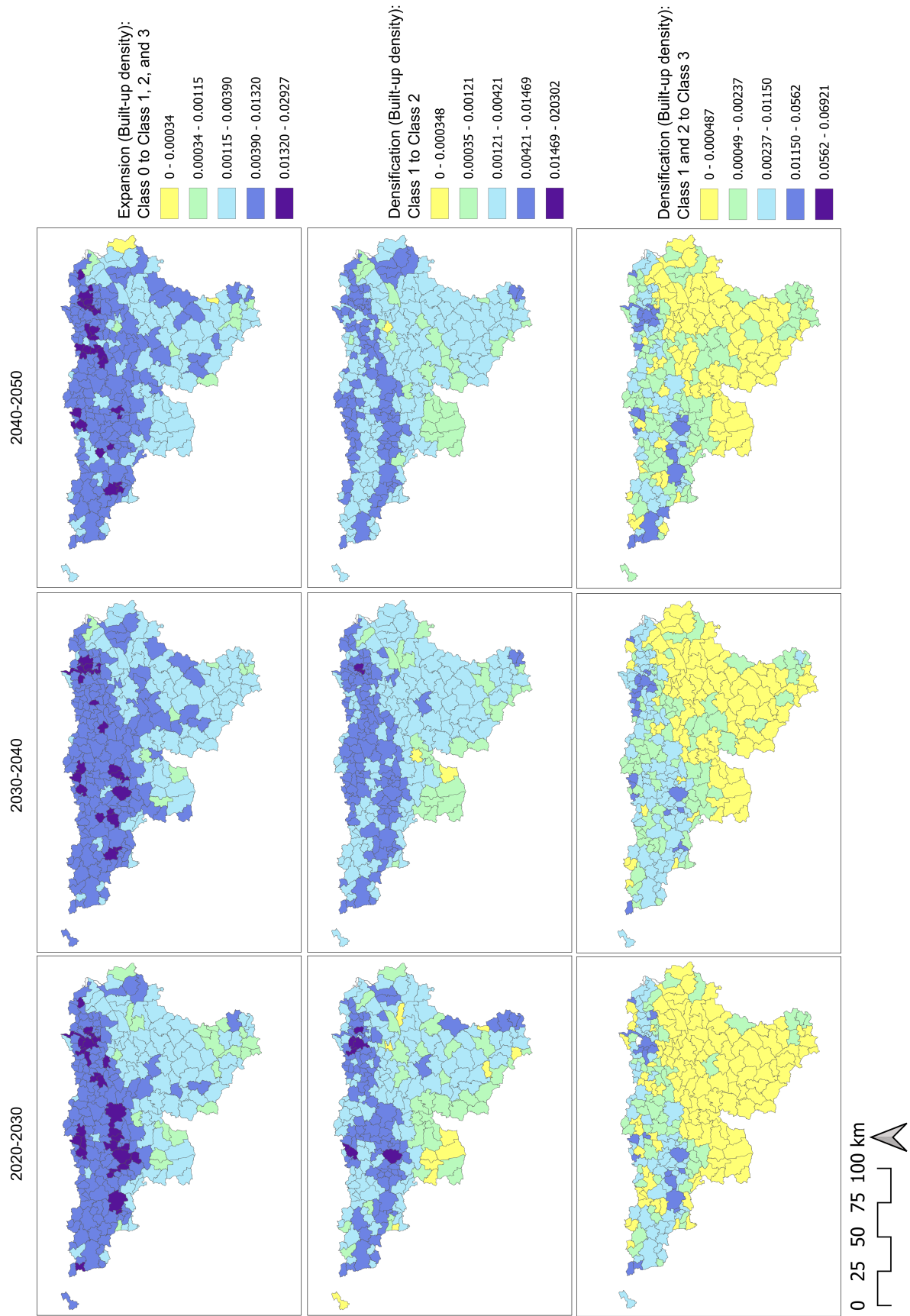


Figure 9: Choropleth map showing spatial distribution of built-up density per municipality for the GAU scenario

## 4 Discussion

The MNL model calibration and validation offer a robust foundation for analysing urban transitions under BAU and GAU scenarios. These results establish confidence in the spatial and temporal dynamics simulated under both scenarios. High calibration accuracy indicates the model’s ability to capture relationships between explanatory variables and land-use changes, while validation ensures reliability by closely matching simulated outputs with observed urban growth. MNL coefficients reveal the relative influence of geophysical, socioeconomic, and zoning variables on urban transitions, aligning with Wallonia’s historical and regulatory context. Geophysical factors like elevation and slope influence development patterns, with flat terrain encouraging low-density areas and rugged topography hindering growth. In addition to the influence of zoning policy, Proximity to employment hubs is also proven to be one of the critical drivers of urban densification. These results depict that Wallonia follows an infrastructure-oriented development similar to (Poelmans and Van Rompaey (2010), Mustafa et al. (2018d), ESPON (2020)). Supporting this, a negative impact of roads and railway stations shows that Belgium do not enforce a transit-oriented development. Despite zoning restrictions, urban expansion in peri-urban areas like Gembloux and Ciney continues due to their strategic location between Brussels and Namur, with commuters seeking affordable housing while maintaining access to employment centres, where major cities and its infrastructure has an influence on the urban growth of its peripheral areas [Figure 8](#) and [Figure 9](#).

The BAU and GAU scenarios reveal distinct urban development trajectories in Wallonia, shaped by regulatory, socioeconomic, and geophysical factors. BAU reflects decreasing land consumption, transitioning toward densification, with urban expansion slowing post-2040, as supported by Mustafa et al. (2018c) and Charliers Julien and Reginster Isabelle (2024). While adaptive local governance policies contribute to compact growth, socioeconomic forces—such as employment accessibility, commuting patterns, and housing demand—also drive densification. High-accessibility locations like Liège, Namur, and Charleroi attract urban intensification, often independent of zoning policies. In contrast, GAU, with weaker regulatory control, fosters suburban sprawl, particularly in municipalities without strong containment measures. The model’s coefficients highlight the historical evolution of land-use transitions and their probable trajectories under both scenarios. While BAU offers an optimistic view, it may oversimplify urbanisation dynamics by underestimating market-driven forces, with GAU providing a necessary counterpoint to capture the risks of unregulated expansion. A balanced approach, integrating both regulatory and market-driven factors, is crucial for accurately modelling future urban growth in Wallonia.

Urban growth under the BAU scenario is more controlled and compact than in GAU, as reflected in spatial metrics. In municipalities like Liège, Namur, and areas near Brussels (e.g., Wavre and Ottignies-Louvain-la-Neuve), a lower USI indicates reduced urban sprawl and increased densification. While policies promoting infill development and limiting outward expansion contribute, market forces play a key role. Housing demand in well-connected employment hubs drives densification, even without strict zoning regulations. Liège, for instance, has intensified due to its transformation into a logistics hub, with the *Trilogiport* inland port and Airport attracting newly built large developments. Consequently, BAU results in fewer but larger and

more cohesive urban patches, with higher AC and lower PD, reflecting improved connectivity. Circular construction and land reuse strategies further support this trend. As shown in [Figure 8](#) and [Figure 9](#), Liège and Namur prioritise densified over outward expansion, reducing land consumption. However, a few patches around the centres of main cities like Liege, Charleroi and Mons experience expansion, which shows that cities attract outward growth. This can be observed in municipalities like Fléron and Ans, which act as a conurbation between two major cities. In contrast, GAU fosters fragmentation, with weaker containment measures enabling uncontrolled suburban sprawl, particularly in peri-urban and rural municipalities.

In peri-urban municipalities like Mons, La Louvière, Arlon, and Bastogne, the BAU scenario fosters controlled growth, with lower USI and higher AC, reducing fragmentation and promoting densification. This results in a more cohesive urban structure and efficient land use. However, rising property prices in central locations, like Brussels, push residents toward suburban areas like Waterloo and Jodoigne, where affordability drives expansion beyond policy-driven densification. For example, Waterloo, known for its high property values and quality of life, attracts affluent commuters, further intensifying suburban growth and increasing pressure on available land. This market-driven dynamic complicates BAU's containment of sprawl. In contrast, GAU leads to fragmented, low-density sprawl, with decreasing AC and increasing USI, reflecting inefficient land use and environmental strain. The stark contrast between BAU and GAU highlights the effectiveness of compact growth strategies under strong regulatory influence and the risks of unchecked expansion when regulations are weak. While BAU supports sustainable urbanisation, external economic pressures must be considered to fully address urban growth dynamics in Wallonia.

The GAU scenario, representing a *laissez-faire* approach of urban growth, is a cautionary view of the potential consequences of uncontrolled urban expansion. Spatial metrics under GAU reveal higher levels of urban sprawl, with municipalities like Charleroi, Liège, and the municipalities of Wallon Barabant. They experience a more extensive development, often spilling into rural and peri-urban areas. This pattern of fragmented growth, with lower AC and higher USI, underscores the risks of an expansionist approach to urban development. The spatial inefficiencies and increased ecological degradation in GAU point to the importance of implementing regulatory measures to control urban sprawl. The GAU scenario serves as a necessary contrast to BAU, providing valuable insights into the potential consequences of inaction in urban planning. While expansion is dominant across Wallonia in the case of GAU, densification is more prominent in and around cities and prosperous municipalities of Walloon Brabant like Wavre, Lasne, Louvain-la-Neuve, etc.

In summary, the comparative analysis of BAU and GAU scenarios highlights the stark differences in urban development patterns for Wallonia. While BAU, shaped by historical trends, emphasises a progressive shift to densification, the GAU is a contrasting scenario which highlights the potential dangers of unchecked growth, with fragmented urban development and increased ecological degradation. These findings underscore the need for integrated strategies that balance urban growth with sustainability. Given the limitations of the BAU scenario—its assumption of continued growth despite real-world challenges—it is crucial to incorporate the GAU scenario into future modelling efforts. The GAU scenario provides an essential perspective

on the potential risks of urban sprawl and the need for comprehensive management. Both scenarios are necessary for a more accurate understanding of potential urban dynamics, with GAU helping to prepare for risks and challenges that may arise from real-world urban development pressures.

## 5 Conclusion

This study developed an MNL-CA model to assess urban growth patterns in Wallonia, Belgium, under two distinct scenarios: Business-As-Usual (BAU) and Growth-As-Usual (GAU). The research aimed to understand urban expansion, densification, and the role of urban policies in managing land take over time.

The findings highlight the inherent limitations of the BAU scenario, which assumes a steady decline in land consumption and the eventual stabilisation of urban expansion by 2040. While BAU projects compact urban growth, it risks underestimating sustained development pressures, such as housing demand and economic growth, potentially leading to overly optimistic planning assumptions. In spatial metrics, BAU revealed more controlled and compact urban growth, with lower Urban Sprawl Index (USI) values, reduced fragmentation, and improved connectivity in urban patches (higher Average Contiguity or AC). However, it risks not fully accounting for persistent urbanisation trends that may continue beyond 2040, possibly leading to spatial inefficiencies in the long run.

In contrast, the GAU scenario served as a necessary stress test, revealing the consequences of unchecked urban expansion. GAU showed higher land consumption, fragmented development patterns, and an increased strain on infrastructure and resources, exposing the vulnerabilities of weak or inconsistent policy enforcement. The spatial metrics under GAU reflected higher USI, lower patch density (PD), and more fragmented urban landscapes, highlighting the challenge of managing urban sprawl. GAU also showed a less efficient land-use structure, with larger urban patches and less cohesion, reinforcing the need for stronger urban containment policies.

Finally, while BAU provides a view of controlled urban growth, GAU is essential for evaluating long-term risks and testing urban policies under persistent expansion pressures. Incorporating GAU-based assessments into urban planning can help design strategies to mitigate urban sprawl and enhance land-use sustainability. Under the GAU scenario, solutions such as densification and the promotion of urban centralities, as proposed by the Spatial Development Strategy (SDT) in Wallonia, will be key in addressing the challenges of No Net Land Take (NNLT) by 2050. These solutions will contribute to more compact, sustainable urban forms that minimise land consumption and facilitate efficient land-use planning.

This research contributes to the broader discourse on urban modelling and sustainable growth, emphasising the importance of scenario-based planning in shaping resilient cities. By balancing realistic expansion scenarios with policy-driven urban containment, planners can develop evidence-based strategies that ensure cities remain economically viable, environmentally sustainable, and capable of addressing future urban challenges.

## Authorship contribution

Anasua Chakraborty: writing – original draft, validation, software, resources, methodology, investigation, formal analysis, data curation, conceptualisation. Ahmed Mustafa: writing – review & editing, software, supervision, and conceptualisation. Lien Poelmans: writing – review, methodology, investigation, conceptualisation. Jacques Teller: writing – review & editing, supervision, investigation, funding acquisition.

## Declaration of conflicting interests

The authors reported no potential conflict of interest.

## Funding

This research was funded by the INTER program and co-funded by the Fond National de la Recherche, Luxembourg (FNR) and the Fund for Scientific Research-FNRS, Belgium (F.R.S—FNRS), T.0233.20—‘Sustainable Residential Densification’ project (SusDens, 2020–2024).

## Data availability

The code supporting this study, along with illustrative examples, is openly available on <https://doi.org/10.5281/zenodo.15163673>

## Acknowledgements

The author(s) would like to express their gratitude to Prabhath Chilakalapudi from the Max Planck Institute of Sustainable Materials, Düsseldorf, for their valuable assistance in coding and the development of the Python package used in this research.

## References

- Al-Ahmadi K, See L, Heppenstall A and Hogg J (2009) Calibration of a fuzzy cellular automata model of urban dynamics in Saudi Arabia. *Ecological Complexity* 6(2): 80–101. DOI:10.1016/J.ECOCOM.2008.09.004. URL <https://doi.org/10.1016/j.ecocom.2008.09.004>.
- Arlinghaus S and Kerski J (2013) Spatial Mathematics : Theory and Practice through Mapping. *Spatial Mathematics* DOI:10.1201/B15049. URL <https://doi.org/10.1201/b15049>.
- Barros CP and Balsas CJL (2020) Luanda’s Slums: An overview based on poverty and gentrification. *Urban Development Issues* 64(1): 29–38. DOI:10.2478/UDI-2019-0021. URL <https://doi.org/10.2478/UDI-2019-0021>.
- Batty M (1997) Cellular Automata and Urban Form: A Primer. *Journal of the American Planning Association* 63(2): 266–274. DOI:10.1080/01944369708975918. URL <https://doi.org/10.1080/01944369708975918>.

- Beckers A, Dewals B, Erpicum S, Dujardin S, Detrembleur S, Teller J, Pirotton M and Archambeau P (2013) Contribution of land use changes to future flood damage along the river Meuse in the Walloon region. *Natural Hazards and Earth System Sciences* 13(9): 2301–2318. DOI: 10.5194/NHESS-13-2301-2013. URL <https://doi.org/10.5194/nhess-13-2301-2013>.
- Broitman D and Koomen E (2015) Residential density change: Densification and urban expansion. *Computers, Environment and Urban Systems* 54: 32–46. DOI:10.1016/J.COMPENVURBSYS.2015.05.006. URL <https://doi.org/10.1016/j.compenvurbsys.2015.05.006>.
- C Montgomery D, A Peck E and Vining GG (2012) Transformation and weighting to correct model inadequacies. In: *Introduction to linear regression analysis*, 5th edition, chapter 5. John Wiley & Sons, Inc. ISBN 978-0-470-54281-1, pp. 171–187. DOI:10.1111/insr.12020\_10. URL [http://doi.org/10.1111/insr.12020\\_10](http://doi.org/10.1111/insr.12020_10).
- Cammerer H, Thielen AH and Verburg PH (2013) Spatio-temporal dynamics in the flood exposure due to land use changes in the Alpine Lech Valley in Tyrol (Austria). *Natural Hazards* 68(3): 1243–1270. DOI:10.1007/S11069-012-0280-8. URL <http://doi.org/10.1007/s11069-012-0280-8>.
- Chakraborty A, Joshi MY, Mustafa A, Cools M and Teller J (2025) Model’s parameter sensitivity assessment and their impact on Urban Densification using regression analysis. *Geography and Sustainability* 6(2): 100276. DOI:10.1016/J.GEOSUS.2025.100276. URL <https://doi.org/10.1016/j.geosus.2025.100276>.
- Chakraborty A, Mustafa A, Omrani H and Teller J (2023) A Framework to Probe Uncertainties in Urban Cellular Automata Modelling Using a Novel Framework of Multilevel Density Approach: A Case Study for Wallonia Region, Belgium. *Urban Book Series Part F270*: 325–341. DOI:10.1007/978-3-031-31746-0\_17. URL [https://doi.org/10.1007/978-3-031-31746-0\\_17](https://doi.org/10.1007/978-3-031-31746-0_17).
- Chakraborty A, Mustafa A and Teller J (2024a) City Planning Dynamics: A Theoretical Framework of Urban Development Scenario of Belgium Provinces Using Logit Based Cellular Automata. In: *GEOProcessing 2024 : The Sixteenth International Conference on Advanced Geographic Information Systems, Applications, and Services*. Barcelona, Spain: IARIA, pp. 14–17. URL [https://www.thinkmind.org/library/GEOProcessing/GEOProcessing\\_2024/geoprocessing\\_2024\\_1\\_40\\_30039.html](https://www.thinkmind.org/library/GEOProcessing/GEOProcessing_2024/geoprocessing_2024_1_40_30039.html).
- Chakraborty A, Mustafa A and Teller J (2024b) Modelling multi-density urban expansion using Cellular Automata for Brussels Metropolitan Development Area. *ISPRS Annals of the Photogrammetry, Remote Sensing and Spatial Information Sciences* X-4/W4-2024: 29–34. DOI:10.5194/ISPRS-ANNALS-X-4-W4-2024-29-2024. URL <https://doi.org/10.5194/isprs-annals-x-4-w4-2024-29-2024>.
- Chakraborty A, Omrani H and Teller J (2022a) A Comparative Analysis of Drivers Impacting Urban Densification for Cross Regional Scenarios in Brussels Metropolitan Area. *Land* 2022, Vol. 11, Page 2291 11(12): 2291. DOI:10.3390/LAND11122291. URL <https://doi.org/10.3390/land11122291>.

- Chakraborty A, Omrani H and Teller J (2022b) Modelling the Drivers of Urban Densification to Evaluate Built-up Areas Extension: A Data-Modelling Solution Towards Zero Net Land Take. *Lecture Notes in Computer Science (including subseries Lecture Notes in Artificial Intelligence and Lecture Notes in Bioinformatics)* 13376 LNCS: 260–270. DOI:10.1007/978-3-031-10450-3\_21. URL [https://doi.org/10.1007/978-3-031-10450-3\\_21](https://doi.org/10.1007/978-3-031-10450-3_21).
- Charliers Julien and Reginster Isabelle (2024) Artificialization of soil, urban sprawl and land availability: where is Wallonia? - Iweps. URL <https://www.iweps.be/wp-content/uploads/2024/09/RS12-Territoire.pdf>.
- Chen G, Li X, Liu X, Chen Y, Liang X, Leng J, Xu X, Liao W, Qiu Y, Wu Q and Huang K (2020) Global projections of future urban land expansion under shared socioeconomic pathways. *Nature Communications* 2020 11:1 11(1): 1–12. DOI:10.1038/s41467-020-14386-x. URL <https://doi.org/10.1038/s41467-020-14386-x>.
- Chen Y, Li X, Liu X and Ai B (2014) Modeling urban land-use dynamics in a fast developing city using the modified logistic cellular automaton with a patch-based simulation strategy. *International Journal of Geographical Information Science* 28(2): 234–255. DOI:10.1080/13658816.2013.831868. URL <https://doi.org/10.1080/13658816.2013.831868>.
- Clarke KC, Hoppen S and Gaydos LJ (1996) Methods and techniques for rigorous calibration of a cellular automaton model of urban growth. In: *Third International Conference/Workshop on Integrating GIS and Environmental Modeling*. Santa Fe, New Mexico: National Center for Geographic Information and Analysis, pp. 1319–1328. URL <https://pubs.usgs.gov/publication/70202456>.
- Colsaet A, Laurans Y and Levrel H (2018) What drives land take and urban land expansion? A systematic review. *Land Use Policy* 79: 339–349. DOI:10.1016/J.LANDUSEPOL.2018.08.017. URL <https://doi.org/10.1016/j.landusepol.2018.08.017>.
- Congalton RG (1991) A review of assessing the accuracy of classifications of remotely sensed data. *Remote Sensing of Environment* 37(1): 35–46. DOI:10.1016/0034-4257(91)90048-B. URL [https://doi.org/10.1016/0034-4257\(91\)90048-B](https://doi.org/10.1016/0034-4257(91)90048-B).
- CPDT (2024) Territorial development plan, Belgium. URL <https://territoire.wallonie.be/storage/territoire/documents/content/page/wallonie-2050/analyse-contextuelle-.pdf>.
- Dewan AM and Yamaguchi Y (2009) Land use and land cover change in Greater Dhaka, Bangladesh: Using remote sensing to promote sustainable urbanization. *Applied Geography* 29(3): 390–401. DOI:10.1016/J.APGEOG.2008.12.005. URL <https://doi.org/10.1016/j.apgeog.2008.12.005>.
- Elmqvist T, Goodness J, Marcotullio PJ, Parnell S, Sendstad M, Wilkinson C, Fragkias M, Güneralp B, McDonald RI, Schewenius M and Seto KC (2013) *Urbanization, biodiversity and ecosystem services: Challenges and opportunities: A global assessment*. Springer Dordrecht.

- ISBN 9789400770881. DOI:10.1007/978-94-007-7088-1. URL <https://doi.org/10.1007/978-94-007-7088-1>.
- ESPON (2020) Territorial patterns and relations in Belgium - Country fiche | ESPON. URL <https://archive.espon.eu/belgium>.
- Esposito P, Patriarca F and Salvati L (2018) Tertiarization and land use change: The case of Italy. *Economic Modelling* 71: 80–86. DOI:10.1016/J.ECONMOD.2017.12.002. URL <https://doi.org/10.1016/j.econmod.2017.12.002>.
- García AM, Santé I, Boullón M and Crecente R (2012) A comparative analysis of cellular automata models for simulation of small urban areas in Galicia, NW Spain. *Computers, Environment and Urban Systems* 36(4): 291–301. DOI:10.1016/J.COMPENVURBSYS.2012.01.001. URL <https://doi.org/10.1016/j.compenvurbsys.2012.01.001>.
- Hanoq P (2011) Territorial planning system and urban development - From a deterministic to a strategic model. *7th International Conference on Virtual Cities and Territories* : 319–325 URL <https://hdl.handle.net/2268/112982>.
- Hosseinali F, Alesheikh AA and Nourian F (2013) Agent-based modeling of urban land-use development, case study: Simulating future scenarios of Qazvin city. *Cities* 31: 105–113. DOI: 10.1016/J.CITIES.2012.09.002. URL <http://doi.org/10.1016/j.cities.2012.09.002>.
- Hu Z and Lo CP (2007) Modeling urban growth in Atlanta using logistic regression. *Computers, Environment and Urban Systems* 31(6): 667–688. DOI:10.1016/J.COMPENVURBSYS.2006.11.001. URL <https://doi.org/10.1016/j.compenvurbsys.2006.11.001>.
- Kasanko M, Barredo JI, Lavalle C, McCormick N, Demicheli L, Sagris V and Brezger A (2006) Are European cities becoming dispersed?: A comparative analysis of 15 European urban areas. *Landscape and Urban Planning* 77(1-2): 111–130. DOI:10.1016/J.LANDURBPLAN.2005.02.003. URL <https://doi.org/10.1016/J.LANDURBPLAN.2005.02.003>.
- Khuri AI (2013) Introduction to Linear Regression Analysis, Fifth Edition by Douglas C. Montgomery, Elizabeth A. Peck, G. Geoffrey Vining. *International Statistical Review* 81(2): 318–319. DOI:10.1111/insr.12020\_10. URL [http://doi.org/10.1111/insr.12020\\_10](http://doi.org/10.1111/insr.12020_10).
- Kim Y and Newman G (2020) Advancing scenario planning through integrating urban growth prediction with future flood risk models. *Computers, Environment and Urban Systems* 82: 101498. DOI:10.1016/J.COMPENVURBSYS.2020.101498. URL <https://doi.org/10.1016/j.compenvurbsys.2020.101498>.
- Lathey V, Guhathakurta S and Aggarwal RM (2009) The Impact of Subregional Variations in Urban Sprawl on the Prevalence of Obesity and Related Morbidity. <http://dx.doi.org/10.1177/0739456X09348615> 29(2): 127–141. DOI:10.1177/0739456X09348615. URL <https://doi.org/10.1177/0739456X09348615>.
- Li X and Yeh AGO (2000) Modelling sustainable urban development by the integration of constrained cellular automata and GIS. *International Journal of Geographical Information*

- Science* 14(2): 131–152. DOI:10.1080/136588100240886. URL <https://doi.org/10.1080/136588100240886>.
- Liu Y, Li L, Chen L, Cheng L, Zhou X, Cui Y, Li H and Liu W (2019) Urban growth simulation in different scenarios using the SLEUTH model: A case study of Hefei, East China. *PLOS ONE* 14(11): e0224998. DOI:10.1371/JOURNAL.PONE.0224998. URL <https://doi.org/10.1371/journal.pone.0224998>.
- Martin H, Couclelis H and Clarke KC (2005) The role of spatial metrics in the analysis and modeling of urban land use change. *Computers, Environment and Urban Systems* 29(4): 369–399. DOI:10.1016/J.COMPENVURBSYS.2003.12.001. URL <https://doi.org/10.1016/j.compenvurbsys.2003.12.001>.
- Mundia CN and Aniya M (2005) Analysis of land use/cover changes and urban expansion of Nairobi city using remote sensing and GIS. *International Journal of Remote Sensing* 26(13): 2831–2849. DOI:10.1080/01431160500117865. URL <https://doi.org/10.1080/01431160500117865>.
- Mustafa A, Bruwier M, Archambeau P, Erpicum S, Piroton M, Dewals B and Teller J (2018a) Effects of spatial planning on future flood risks in urban environments. *Journal of Environmental Management* 225: 193–204. DOI:10.1016/J.JENVMAN.2018.07.090. URL <https://doi.org/10.1016/j.jenvman.2018.07.090>.
- Mustafa A, Heppenstall A, Omrani H, Saadi I, Cools M and Teller J (2018b) Modelling built-up expansion and densification with multinomial logistic regression, cellular automata and genetic algorithm. *Computers, Environment and Urban Systems* 67: 147–156. DOI:10.1016/J.COMPENVURBSYS.2017.09.009. URL <https://doi.org/10.1016/j.compenvurbsys.2017.09.009>.
- Mustafa A, Saadi I, Cools M and Teller J (2018c) Understanding urban development types and drivers in Wallonia: A multi-density approach. *International Journal of Business Intelligence and Data Mining* 13(1-3): 309–330. DOI:10.1504/IJBIDM.2018.088434. URL <http://doi.org/10.1504/IJBIDM.2017.10004788>.
- Mustafa A, Van Rompaey A, Cools M, Saadi I and Teller J (2018d) Addressing the determinants of built-up expansion and densification processes at the regional scale. *Urban Studies* 55(15): 3279–3298. DOI:10.1177/0042098017749176. URL <https://doi.org/10.1177/0042098017749176>.
- Naikoo MW, Shahfahad, Talukdar S, Ishtiaq M and Rahman A (2023) Modelling built-up land expansion probability using the integrated fuzzy logic and coupling coordination degree model. *Journal of Environmental Management* 325: 116441. DOI:10.1016/J.JENVMAN.2022.116441. URL <https://doi.org/10.1016/j.jenvman.2022.116441>.
- OpenStreetMap Foundation contributors (2024) OpenStreetMap. URL <https://www.openstreetmap.org/#map=8/50.510/4.475>.

- Overmars KP, De Koning GH and Veldkamp A (2003) Spatial autocorrelation in multi-scale land use models. *Ecological Modelling* 164(2-3): 257–270. DOI:10.1016/S0304-3800(03)00070-X. URL [https://doi.org/10.1016/S0304-3800\(03\)00070-X](https://doi.org/10.1016/S0304-3800(03)00070-X).
- Poelmans L and Van Rompaey A (2009) Detecting and modelling spatial patterns of urban sprawl in highly fragmented areas: A case study in the Flanders–Brussels region. *Landscape and Urban Planning* 93(1): 10–19. DOI:10.1016/J.LANDURBPLAN.2009.05.018. URL <https://doi.org/10.1016/j.landurbplan.2009.05.018>.
- Poelmans L and Van Rompaey A (2010) Complexity and performance of urban expansion models. *Computers, Environment and Urban Systems* 34(1): 17–27. DOI:10.1016/j.compenvurbsys.2009.06.001. URL <https://doi.org/10.1016/j.compenvurbsys.2009.06.001>.
- Pontius GR and Schneider LC (2001) Land-cover change model validation by an ROC method for the Ipswich watershed, Massachusetts, USA. *Agriculture, Ecosystems & Environment* 85(1-3): 239–248. DOI:10.1016/S0167-8809(01)00187-6. URL [https://doi.org/10.1016/S0167-8809\(01\)00187-6](https://doi.org/10.1016/S0167-8809(01)00187-6).
- Public service of Wallonia (2020) Téléchargement des données | Géoportail de la Wallonie. URL <https://geoportail.wallonie.be>.
- Rienow A and Goetzke R (2015) Supporting SLEUTH – Enhancing a cellular automaton with support vector machines for urban growth modeling. *Computers, Environment and Urban Systems* 49: 66–81. DOI:10.1016/J.COMPENVURBSYS.2014.05.001. URL <https://doi.org/10.1016/j.compenvurbsys.2014.05.001>.
- Rwanga SS, Ndambuki JM, Rwanga SS and Ndambuki JM (2017) Accuracy Assessment of Land Use/Land Cover Classification Using Remote Sensing and GIS. *International Journal of Geosciences* 8(4): 611–622. DOI:10.4236/IJG.2017.84033. URL <https://doi.org/10.4236/ijg.2017.84033>.
- Seto KC, Fragkias M, Güneralp B and Reilly MK (2011) A Meta-Analysis of Global Urban Land Expansion. *PLoS ONE* 6(8): e23777. DOI:10.1371/JOURNAL.PONE.0023777. URL <https://doi.org/10.1371/journal.pone.0023777>.
- Silva EA and Clarke KC (2002) Calibration of the SLEUTH urban growth model for Lisbon and Porto, Portugal. *Computers, Environment and Urban Systems* 26(6): 525–552. DOI:10.1016/S0198-9715(01)00014-X. URL [https://doi.org/10.1016/S0198-9715\(01\)00014-X](https://doi.org/10.1016/S0198-9715(01)00014-X).
- SPW (2017) Report on the state of the Walloon environment 2017 - State of the Walloon environment. Technical report, Service public de Wallonie;Département de l'étude du milieu naturel et agricole;DGO3 - Direction générale des ressources naturelles, de l'agriculture et de l'environnement. URL <https://etat.environnement.wallonie.be/contents/publications/rapport-sur-letat-de-lenvironnement-wallon-2017.html>.
- Statbel (2017) About Statbel | Statbel. URL <https://statbel.fgov.be/en/about-statbel>.

- Tang Z, Engel BA, Pijanowski BC and Lim KJ (2005) Forecasting land use change and its environmental impact at a watershed scale. *Journal of Environmental Management* 76(1): 35–45. DOI:10.1016/J.JENVMAN.2005.01.006. URL <https://doi.org/10.1016/J.JENVMAN.2005.01.006>.
- Thorne JH, Santos MJ and Bjorkman JH (2013) Regional Assessment of Urban Impacts on Landcover and Open Space Finds a Smart Urban Growth Policy Performs Little Better than Business as Usual. *PLOS ONE* 8(6): e65258. DOI:10.1371/JOURNAL.PONE.0065258. URL <https://doi.org/10.1371/journal.pone.0065258>.
- Ullah and Ibrar (2022) Re-identifying the Rural/Urban: A case Study of Pakistan. *Espaço e Economia* 11(23). DOI:10.4000/ESPACOECONOMIA.22019. URL <https://doi.org/10.4000/espacoeconomia.22019>.
- United Nations (2018) The World’s Cities in 2018 Data Booklet | Population Division. URL <https://www.un.org/development/desa/pd/content/worlds-cities-2018-data-booklet>.
- Vermeiren K, Van Rompaey A, Loopmans M, Serwajja E and Mukwaya P (2012) Urban growth of Kampala, Uganda: Pattern analysis and scenario development. *Landscape and Urban Planning* 106(2): 199–206. DOI:10.1016/J.LANDURBPLAN.2012.03.006. URL <http://doi.org/10.1016/j.landurbplan.2012.03.006>.
- Waddell P (2002) UrbanSim: Modeling Urban Development for Land Use, Transportation, and Environmental Planning. *Journal of the American Planning Association* 68(3): 297–314. DOI:10.1080/01944360208976274. URL <https://doi.org/10.1080/01944360208976274>.
- Wang S, Zheng X and Zang X (2012) Accuracy assessments of land use change simulation based on Markov-cellular automata model. *Procedia Environmental Sciences* 13: 1238–1245. DOI: 10.1016/j.proenv.2012.01.117. URL <http://doi.org/10.1016/j.proenv.2012.01.117>.
- Wang YP and Kintrea K (2021) Urban Expansion and Land Use Changes in Asia and Africa. *Environment and Urbanization ASIA* 12(1\_suppl): S13–S17. DOI:10.1177/0975425321999081. URL <https://doi.org/10.1177/0975425321999081>.
- White R and Engelen G (1997) Cellular Automata as the Basis of Integrated Dynamic Regional Modelling. *Environment and Planning B* 24(2): 235–246. DOI:10.1068/B240235. URL <https://doi.org/10.1068/b240235>.
- White R and Engelen G (2000) High-resolution integrated modelling of the spatial dynamics of urban and regional systems. *Computers, Environment and Urban Systems* 24(5): 383–400. DOI:10.1016/S0198-9715(00)00012-0. URL [https://doi.org/10.1016/S0198-9715\(00\)00012-0](https://doi.org/10.1016/S0198-9715(00)00012-0).
- Zaitsev DA (2017) A generalized neighborhood for cellular automata. *Theoretical Computer Science* 666: 21–35. DOI:10.1016/J.TCS.2016.11.002. URL <https://doi.org/10.1016/j.tcs.2016.11.002>.

Zhang B and Wang H (2021) A new type of dual-scale neighborhood based on vectorization for cellular automata models. *GIScience and Remote Sensing* 58(3): 386–404. DOI:10.1080/15481603.2021.1883946. URL <https://doi.org/10.1080/15481603.2021.1883946>.

## Supplementary material

Table 8: MNL coefficients for variables across class to class transitions for the years 2000-2010

| Name                            | Abbreviation | Coefficients for Class to Class Transitions |         |         |         |         |         |
|---------------------------------|--------------|---|---------|---------|---------|---------|---------|
|                                 |              | 0 to 1                                      | 0 to 2  | 0 to 3  | 1 to 2  | 1 to 3  | 2 to 3  |
| Elevation                       | DEM          | 0.042                                       | -0.016  | *-0.152 | *0.098  | -0.032  | -0.060  |
| Slope                           | SL           | *-0.091                                     | *-0.428 | *-1.119 | *-0.149 | *-0.725 | *-0.503 |
| Distance to Road 1              | ER1          | -0.013                                      | *-0.174 | *-0.831 | *-0.079 | -0.266  | *-0.214 |
| Distance to Road 2              | ER2          | 0.020                                       | *-0.106 | *-0.403 | -0.036  | *-0.292 | *-0.134 |
| Distance to Road 3              | ER3          | *-0.147                                     | *-0.255 | *-0.279 | -0.008  | *-0.369 | *-0.090 |
| Distance to Road 4              | ER4          | *-0.361                                     | *-0.317 | -0.113  | -0.031  | -0.226  | *-0.127 |
| Distance to Railway Stations    | ERS          | 0.043                                       | 0.028   | *-0.262 | 0.027   | 0.031   | -0.038  |
| Distance to Large Sized Cities  | ELC          | *-0.036                                     | 0.001   | *0.216  | 0.038   | 0.117   | *0.074  |
| Distance to Medium Sized Cities | EMC          | -0.007                                      | -0.027  | 0.045   | *-0.065 | -0.147  | -0.033  |
| Employment Density              | Den-EMD      | *-0.114                                     | 0.050   | *0.171  | *-0.057 | *0.177  | *0.144  |
| Population                      | POP          | 0.000                                       | *0.000  | *0.000  | 0.000   | 0.000   | 0.000   |
| Zoning                          | ZON          | *3.450                                      | *3.035  | *3.374  | *2.193  | *0.745  | *0.657  |

\*Variable is significant at a p-value < 0.01

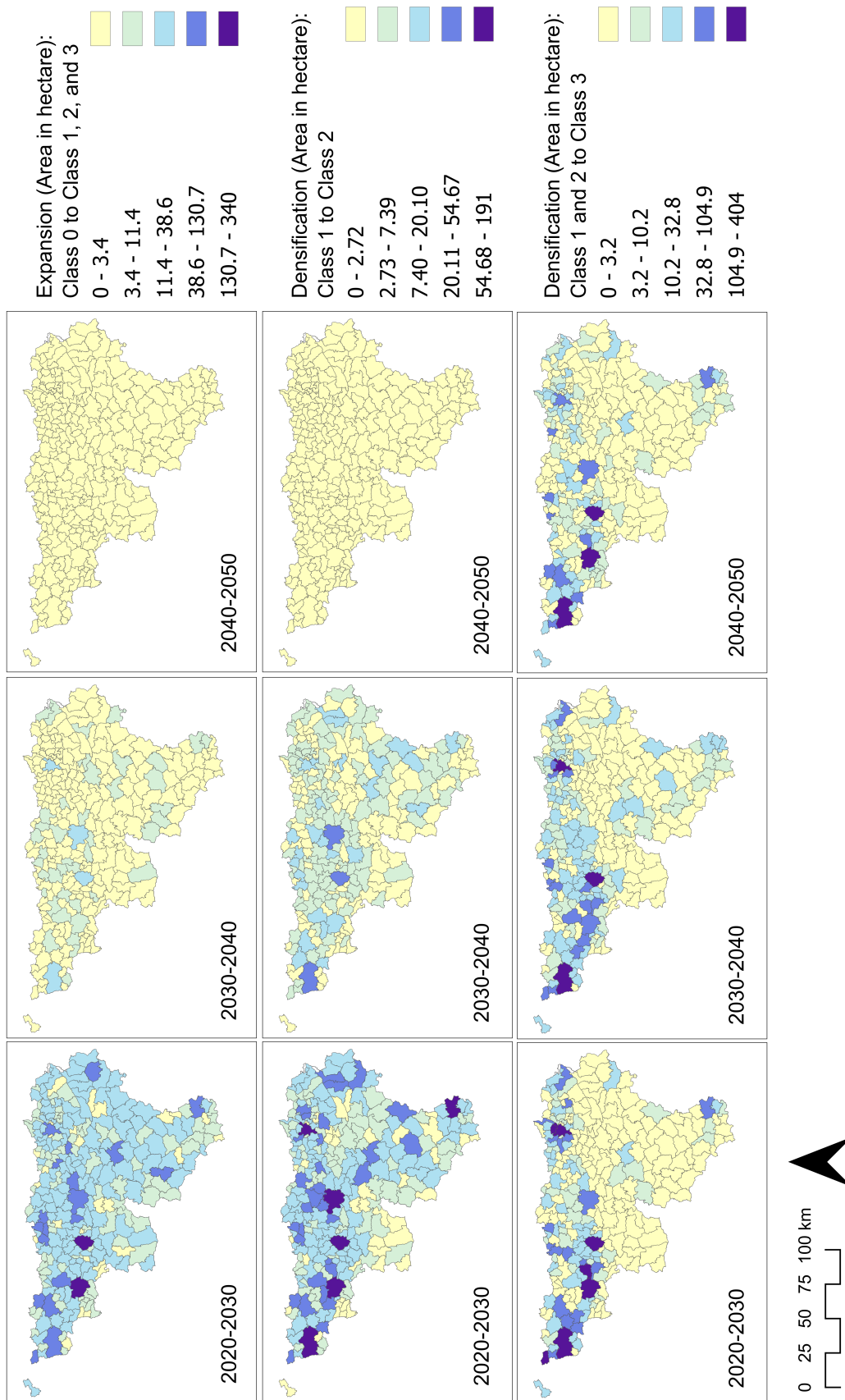


Figure 10: Municipality-wise choropleth map of built-up area for the BAU scenario

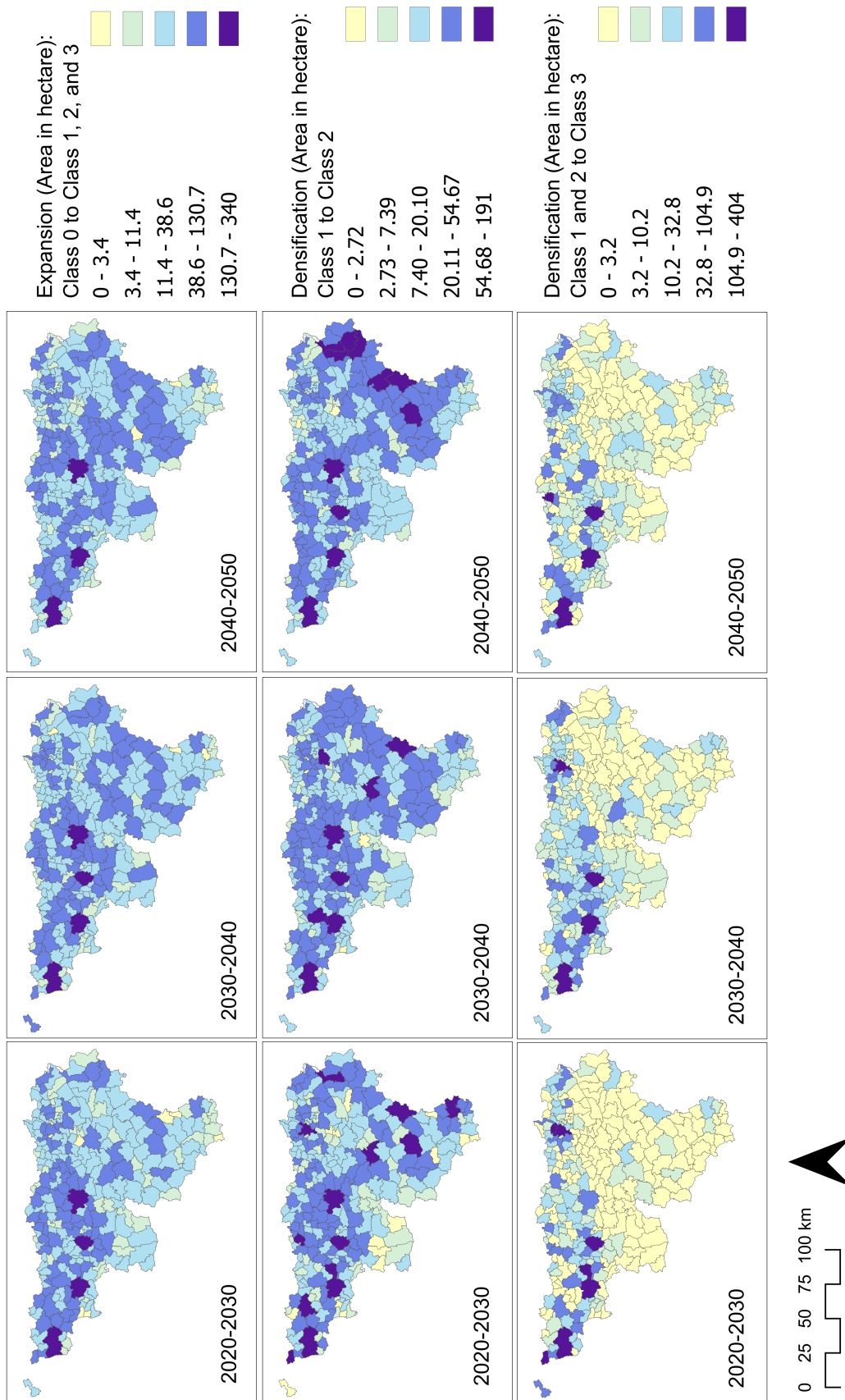


Figure 11: Municipality-wise choropleth map of built-up area for the GAU scenario